2018

Regulatory effects of simvastatin and apoJ on APP processing and amyloid-β clearance in blood-brain barrier endothelial cells

Martina Zandl-Lang
Medical University of Graz

Elham Fanaee-Danesh
Medical University of Graz

Yidan Sun
Medical University of Graz

Nicole Albrecher
Medical University of Graz

Chaitanya Chakravarthi Gali
Medical University of Graz

See next page for additional authors

Publication Details

Zandl-Lang, M., Fanaee-Danesh, E., Sun, Y., Albrecher, N. M., Gali, C., Cancar, I., Kober, A., Tam-Amersdorfer, C., Stracke, A., Storck, S. M., Saeed, A., Stefulj, J., Pietrzik, C. U., Wilson, M. R., Björkhem, I. & Panzenboeck, U. (2018). Regulatory effects of simvastatin and apoJ on APP processing and amyloid-β clearance in blood-brain barrier endothelial cells. Biochimica et Biophysica Acta - Molecular and Cell Biology of Lipids, 1863 (1), 40-60.

Regulatory effects of simvastatin and apoJ on APP processing and amyloid-β clearance in blood-brain barrier endothelial cells

Abstract

Amyloid-β peptides (Aβ) accumulate in cerebral capillaries indicating a central role of the blood-brain barrier (BBB) in the pathogenesis of Alzheimer's disease (AD). Although a relationship between apolipoprotein-, cholesterol- and Aβ metabolism is evident, the interconnecting mechanisms operating in brain capillary endothelial cells (BCEC) are poorly understood. ApoJ (clusterin) is present in HDL that regulates cholesterol metabolism which is disturbed in AD. ApoJ levels are increased in AD brains and in plasma of cerebral amyloid angiopathy (CAA) patients. ApoJ may bind, prevent fibrillization, and enhance clearance of Aβ. We here define a connection of apoJ and cellular cholesterol homeostasis in amyloid precursor protein (APP) processing/Aβ metabolism at the BBB. Silencing of apoJ in primary porcine (p)BCEC decreased intracellular APP and Aβ oligomer levels while the addition of purified apoJ to pBCEC increased intracellular APP and enhanced Aβ clearance across the pBCEC monolayer. Treatment of pBCEC with $Aβ_{(1-40)}$ increased expression of apoJ and receptors involved in amyloid transport including lipoprotein receptor-related protein 1 [LRP1]. In accordance, cerebromicrovascular endothelial cells isolated from 3 x Tg AD mice showed elevated expression levels of apoJ and LRP1 as compared to Non-Tg animals. Treatment of pBCEC with HMGCoA-reductase inhibitor simvastatin markedly increased intracellular and secreted apoJ levels, in parallel increased secreted Aβ oligomers and reduced Aβ uptake and cell-associated Aβ oligomers. Simvastatin effects on apoJ, APP processing, and LRP1 expression in BCEC were confirmed in the mouse model. We suggest a close and complex interaction of apoJ, cholesterol homeostasis, and APP/Aβ processing and clearance at the BBB.

Disciplines

Medicine and Health Sciences

Publication Details

Zandl-Lang, M., Fanaee-Danesh, E., Sun, Y., Albrecher, N. M., Gali, C., Cancar, I., Kober, A., Tam-Amersdorfer, C., Stracke, A., Storck, S. M., Saeed, A., Stefulj, J., Pietrzik, C. U., Wilson, M. R., Björkhem, I. & Panzenboeck, U. (2018). Regulatory effects of simvastatin and apoJ on APP processing and amyloid-β clearance in blood-brain barrier endothelial cells. Biochimica et Biophysica Acta - Molecular and Cell Biology of Lipids, 1863 (1), 40-60.

Authors

Martina Zandl-Lang, Elham Fanaee-Danesh, Yidan Sun, Nicole Albrecher, Chaitanya Chakravarthi Gali, Igor Cancar, Alexandra Kober, Carman Tam-Amersdorfer, Anika Stracke, Steffen Storck, Ahmed Saeed, Jasminka Stefulj, Claus Pietrzik, Mark R. Wilson, Ingemar Björkhem, and Ute Panzenboeck

Regulatory effects of simvastatin and apoJ on APP processing and amyloid-β clearance in blood-brain barrier endothelial cells

Martina Zandl-Lang[1], Elham Fanaee-Danesh[1], Yidan Sun[1], Igor Čančar[1], Chaitanya Chakravarthi Gali[1], Alexandra Kober[1], Nicole M Albrecher[1], Carmen Tam-Amersdorfer[1], Anika Stracke[1], Steffen Storck[2], Ahmed Saeed[3], Jasminka Stefulj[4], Claus Pietrzik[2], Mark R Wilson[5], Ingemar Björkhem[3], Ute Panzenboeck[1*]

[1]Institute of Pathophysiology and Immunology, Medical University of Graz, Austria

[2]Molecular Neurodegeneration, Institute of Pathobiochemistry, University Medical Center of the Johannes Gutenberg-University, Mainz, Germany

[3]Division of Clinical Chemistry, Department of Laboratory Medicine, Karolinska University Hospital, Karolinska Institute Huddinge, Huddinge, Sweden

[4]Laboratory of Neurochemistry and Molecular Neurobiology, Division of Molecular Biology, Rudjer Boskovic Institute, Zagreb, Croatia

[5]School of Biological Sciences, Illawarra Health and Medical Research Institute, University of Wollongong, Wollongong, NSW, Australia

*To whom correspondence should be addressed: Assoc.-Prof. Ute Panzenboeck, Institute of Pathophysiology and Immunology, Medical University of Graz, Heinrichstrasse 31a, 8010 Graz, Austria, Telephone: +433163801955, Fax: +433163809640, E-mail: ute.panzenboeck@medunigraz.at

Highlights:

- Simvastatin shifts APP processing towards the non-amyloidogenic pathway in pBCEC
- Inhibition of cholesterol synthesis by simvastatin up-regulates apoJ in pBCEC
- Both, simvastatin and apoJ increase expression of APP and reduce Aβ uptake in pBCEC
- Increased Aβ and simvastatin induce LRP1 and apoJ levels *in vitro* and *in vivo*
- Thereby clearance of Aβ across the blood-brain barrier is facilitated

Keywords: Alzheimer disease, amyloid-beta (Aβ), endothelium, cholesterol metabolism, blood-brain barrier, clusterin/apoJ

ABSTRACT

Amyloid-β peptides (Aβ) accumulate in cerebral capillaries indicating a central role of the blood-brain barrier (BBB) in the pathogenesis of Alzheimer's disease (AD). Although a relationship between apolipoprotein-, cholesterol- and Aβ metabolism is evident, the interconnecting mechanisms operating in brain capillary endothelial cells (BCEC) are poorly understood. ApoJ (clusterin) is present in HDL that regulates cholesterol metabolism which is disturbed in AD. ApoJ levels are increased in AD brains and in plasma of cerebral amyloid angiopathy (CAA) patients. ApoJ may bind, prevent fibrillization, and enhance clearance of Aβ. We here define a connection of apoJ and cellular cholesterol homeostasis in amyloid precursor protein (APP) processing/Aβ metabolism at the BBB. Silencing of apoJ in primary porcine (p)BCEC decreased intracellular APP and Aβ oligomer levels while the addition of purified apoJ to pBCEC increased intracellular APP and enhanced Aβ clearance across the pBCEC monolayer. Treatment of pBCEC with $Aβ_{(1-40)}$ increased expression of apoJ and receptors involved in amyloid transport including lipoprotein receptor-related protein 1 (LRP1). In accordance, cerebromicrovascular endothelial cells isolated from 3xTg AD mice showed elevated expression levels of apoJ and LRP1 as compared to Non-Tg animals. Treatment of pBCEC with HMGCoA-reductase inhibitor simvastatin markedly increased intracellular and secreted apoJ levels, in parallel increased secreted Aβ oligomers and reduced Aβ uptake and cell-associated Aβ oligomers. Simvastatin effects on apoJ, APP processing, and LRP1 expression in BCEC were confirmed in the mouse model. We suggest a close and complex interaction of apoJ, cholesterol homeostasis, and APP/Aβ processing and clearance at the BBB.

1. INTRODUCTION

Over the past 20 years extensive research and effort has been put into understanding the mechanisms and biochemical pathways underlying Alzheimer's Disease (AD). To date there are two known main pathological hallmarks in the development of the disease (1): (i) abnormally phosphorylated tau proteins forming intracellular neurofibrillary tangles and (ii) deposits of differently sized amyloid beta peptides (Aβ) which oligomerize and form extracellular amyloid plaques surrounded by dystrophic neurites and microglia (2,3). In the last decade it became increasingly evident that AD patients display biochemical, morphological and functional changes in the cerebrovasculature caused by Aβ deposition in arteries and arterioles, but also in capillaries (4–6). This accumulation of Aβ within the walls of cerebral capillaries may trigger capillary cerebral amyloid angiopathy (CAA) (7), which may cause brain hypoperfusion that further stimulates Aβ production (8), altogether implying

a thus far underestimated role of the blood-brain barrier (BBB) in the (early) pathogenesis of AD.

Among various hypotheses of AD development, the amyloid cascade hypothesis, suggesting the formation of amyloid plaques from Aβ peptides, receives the most attention (9,10). The amyloid precursor protein (APP) is processed by two competing pathways, the non-amyloidogenic and the Aβ generating pathway. Sequential cleavage of the transmembrane protein APP by caspase-like enzymes β-secretase (BACE-1) and γ-secretase leads to formation of C-terminal fragment β (CTFβ) and neurotoxic Aβ peptides. Alternatively and prevailing under normal physiological conditions, APP is processed by α-secretase (ADAM10) followed by γ-secretase to form CTFα and cellular secretion of the non-amyloidogenic and neuroprotective sAPPα fragment.

Martins *et al.* reported that AD and atherosclerosis patients reveal similar lipoprotein and cholesterol profiles (11). It appears strikingly that high levels of plasma cholesterol and LDL in mid life (12) and particularly low levels of high-density lipoproteins (HDL) and apolipoprotein (apo)A-I significantly correlate with the development and progression of AD (13). Bates *et al.* described that high HDL serum levels correlate with improved verbal learning and memory performance (14). Cholesterol metabolism in the brain, however, is separated from that in other parts of the body (15). HMGCo-A reductase is the rate-limiting enzyme in cholesterol synthesis, which can be pharmacologically inhibited by statins (16). Unlike most other statins, part of simvastatin in the circulation is able to cross the BBB (17). Although the use of statins in AD remains controversial, beneficial effects of simvastatin treatment on amyloidosis and Aβ plaque load have been observed in several *in vivo* studies (18–21). In addition, recent studies reported beneficial effects of statin treatment explicitly at the BBB, where simvastatin was shown to ameliorate cerebrovascular integrity (22).

Continuous removal of Aβ from the brain is crucial to prevent the development of amyloid plaques and the progression of AD. Aβ peptides can be removed from the brain through various clearing mechanisms (23). Soluble Aβ can be either taken up by microglia and astrocyte phagocytosis. Another way is through brain interstitial fluid (ISF) bulk flow clearance, which involves CSF sink and perivascular clearance mechanisms. However, the majority of Aβ peptides appear to be removed through active transport across the BBB, thus representing the most important clearance pathway (24). A range of receptors have been identified to be involved in uptake and transport of Aβ fragments across the BBB. Among others, receptor for advanced glycation end products (RAGE) and low-density lipoprotein receptor-related protein 1 (LRP1) are proposed to be the major receptors responsible for the

transport of Aβ from the plasma and the brain parenchymal side across the BBB, respectively (25). The outcome of recent studies suggests a link between LRP1 expression and CAA (26). The 600 kDa LRP1 precursor protein is synthesized and subsequently cleaved in the endoplasmic reticulum and golgi-apparatus (27). LRP1 consists of an α- (515 kDa) and a transmembrane β- (85 kDa) chain, which can be further cleaved by metalloproteinases, like ADAM10, and secretases, like BACE1, to generate soluble LRP1 (sLRP1) (28,29). Since sLRP1 is mainly present in the circulation it has been suggested to be the main carrier of Aβ in plasma (25). sLRP1 has been also linked to lipid metabolism and the formation and release of sLRP1 in vascular cells is hypothesized to be stimulated by hypercholesterolemia (30).

Lipoproteins detected in the central nervous system (CNS) reveal a density similar to HDL (31,32). Besides its major task to eliminate excess tissue cholesterol through reverse cholesterol transport mediated by specific ATP binding cassette (ABC) transporters, HDL is also able to bind Aβ and clear the peptides across the BBB. The most abundant apolipoprotein - and most well-known genetic risk factor for AD - is apolipoprotein E (apoE) that also associates with HDL-like particles in the brain (33). ApoE functions as the major cholesterol carrier (followed by apoA-I) regulating lipid homeostasis and thereby mediating lipid transport from one tissue or cell type to another (34). Brain apoE is mainly produced by astrocytes and supports cholesterol transport to neurons via binding to a number of receptors of the LDL receptor family (34). Genome-wide association studies have identified 3 alleles of apoE (ε2, ε3, ε4) with the ε4 allele of APOE as the strongest genetic risk factor for AD affecting Aβ aggregation and clearance (34). Next to apoE and apoA-I, apoJ, also known as clusterin, is among the major apolipoproteins associated with brain HDL-like particles (35,36). ApoJ is an ubiquitously expressed protein firstly described in 1983 in ram rete testis fluid (37). Although highest expression levels of apoJ were detected in brain, only a few studies have investigated its physiological behaviour in the brain. Next to its role in lipid/cholesterol transport and trafficking in the brain (38), apoJ reveals a chaperone function (39). Two independent genome-wide association studies identified gene encoding apoJ in addition to the well-established apoE4 gene, as a novel susceptibility locus for late-onset AD (40,41). ApoJ expression was reported to be increased in AD, especially in neuritic plaques and cerebrovascular deposits (36). A recent study reported increased plasma apoJ levels in CAA patients as compared to AD patients or controls (42). ApoJ is able to avidly bind Aβ, prevent their fibrillization, and enhances Aβ endocytosis by glial cells (36). Importantly, Zlokovic *et al*. revealed that upon binding to apoJ, Aβ peptides can be cleared across the BBB via binding to glycoprotein 330 or megalin receptors (LRP2) (43).

We earlier reported that primary porcine brain capillary endothelial cells (pBCEC) express all key enzymes involved in APP processing, i.e. α-, β-, and γ-secretases, that pBCEC synthesize APP, sAPPα, and Aβ (oligomers), and that modulation of cellular cholesterol metabolism by liver-X receptor (LXR) ligands or cholesterol modulates APP processing in BCEC (44). The goal of the present study was to establish the role of apoJ in cholesterol and Aβ metabolism in cerebromicrovascular endothelial cells by using both a well-established *in vitro* model consisting of primary, porcine BCEC, as well as murine BCEC isolated from 3xTg AD model mice or Non-Tg controls after simvastatin treatment. We here demonstrate that cholesterol homeostasis in BCEC, APP processing, Aß clearance, and expression and secretion of apoJ are complexly linked and influence each other at the level of the BBB.

2. MATERIALS AND METHODS

2.1. Materials

Cell culture flasks, plates, and other plasticware were purchased from Greiner Bio-One (Kremsmünster, Austria). Cell culture medium M199 and MCDB131, minimal essential medium, DMEM/F-12 (Ham's), porcine serum, and dispase were purchased from Life technologies; collagen G from bovine calf skin was obtained from Biochrom (Berlin, Germany), and cell culture additives were from PAA laboratories (Pasching, Austria). Collagenase/dispase was from Roche Applied Science. Transwell multiwell plates (polyester membrane inserts, 0.4 µm pore size) as well as simvastatin, cholesterol, hydrocortisone, Percoll (pH 8.5- 9.5) and $A\beta_{(1-40)}$ (D-A-E-F-R-H-D-S-G-Y-E-V-H-H-Q-K-L-V-F-F-A-E-D-V-G-S-N-K-G-A-I-I-G-L-M-V-G-G-V-V; ≥90% (HPLC)) were purchased from Sigma-Aldrich. 24*(S)*-hydroxycholesterol was purchased from Medical Isotopes (Pelham, Canada), 27-hydroxycholesterol from Avanti Polar Lipids, Inc., and TO901317 from Cayman Chemicals. Dextran was purchased from VWR. [^{14}C]-sucrose, Ultima Gold scintillation cocktail, and scintillation vials were purchased from Perkin Elmer. [^{125}I]-amyloid β peptide $_{(1-40)}$ was obtained from Phoenix Pharmaceuticals. Small interfering RNAs (siRNA) targeting for apoJ were from Microsynth (Switzerland). siRNA transfection reagents were obtained from Lonza, and negative siRNA control from Dharmacon. Polyvinylidene fluoride (PVDF; 0.45 µm) transfer membranes were purchased from GE healthcare. Antibodies used for *in vitro* studies were obtained from Sigma-Aldrich (β-actin Cat#A2066, goat anti-mouse-HRP Cat#A0168), Invitrogen (Rabbit anti-β-Amyloid Precursor Protein Cat#51-2700), Millipore (A11 rabbit anti-Amyloid Oligomer, aβ, oligomeric, Cat# AB9234), Biolegend (Purified anti-β-Amyloid, 1-16 Antibody, Clone:6E10, Cat# 803002) Cloud-Clone Corp. (Polyclonal Antibody to Clusterin (CLU), PAB180Po01) and Santa Cruz Biotechnology (goat anti-rabbit IgG-HRP, Cat# sc-

2030). Antibodies raised against various LRP1 fragments were obtained from AG Pietrzik, Johannes-Gutenberg-University Mainz, Germany. For immunoblot analysis of mBCEC, primary antibodies were purchased from Sigma-Aldrich (Anti- Amyloid Precursor Protein, C-Terminal, Cat#A8717) and from Santa Cruz Biotechnology (clusterin/apoJ (H-330), Cat# sc-8354). Simvastatin used for animal studies was purchased from MSD Austria. PCR reagents were from Bio-Rad and primers were purchased from Invitrogen. Pre-validated primers were purchased from Qiagen (QuantiTect Primer Assay). All other reagents and chemicals were purchased either from Sigma-Aldrich or Merck.

2.2. Isolation and culture of porcine brain capillary endothelial cells (pBCEC)

pBCEC were isolated from 3 hemispheres of freshly slaughtered pigs from the local abattoir (45). Forceps were used to remove meninges and capillaries. A scalpel and a cutter with rolling plates were used to mince the grey and white matter of the brain cortex. To isolate the capillaries, dispase (70 mg/brain) was mixed with 40 ml M199 medium (containing 1% penicillin/streptomycin, 1% gentamycin, 1 mM L-glutamine) and incubated at 37°C in the water bath for 1 h with gentle stirring. 150 ml dextran solution was added and the suspension was centrifuged (6,800xg, 10 min, 4°C). The pellet was resuspended in M199 medium (containing 1% penicillin/streptomycin, 1% gentamycin, 1 mM L-glutamine and 10% porcine serum) and the capillaries were disrupted mechanically by filtering the suspension through a nylon mesh and enzymatically by adding 350 µl collagenase/dispase. The suspension was carefully pipetted onto a Percoll bi-phase gradient (15 ml of 1.07 g/ml Percoll solution on bottom, 20 ml of 1.03 g/ml Percoll solution on top) and centrifuged (1300xg, 10 min) in a swinging bucket rotor. Endothelial cells were isolated from the interphase by aspiration and cells were plated on to collagen coated 75 cm^2 cell culture flasks in M199 medium (containing 1% penicillin/streptomycin, 1% gentamycin, 1 mM L-glutamine, and 10% porcine serum). After 26 h of incubation, endothelial cells were washed twice with PBS and cultured in M199 (containing 1% penicillin/streptomycin, 1 mM L-glutamine and 10% porcine serum) until confluent. Confluent cells were trypsinized and split onto collagen-coated multiwell plates (60 µg/ml collagen) or transwells (120 µg/ml collagen) for further experiments. All cell culture incubations were performed at 37°C in humidified air containing 5% CO_2.

2.3. Activation of simvastatin

Before simvastatin was used in *in vitro* cell culture experiments, it was activated by opening the lactone ring. Activation was performed according to the protocol provided by Merck (46,47). In brief, 1 mg of simvastatin was dissolved in 0.1 ml of absolute ethanol and subsequent addition of 150 µl 0.1 N NaOH. The solution was heated at 50 °C for 2 h and

neutralized to pH 7.2 with 1 N HCl. The solution was brought to a final volume of 4 mg/ml with distilled water and stored at –20 °C until use.

2.4. Transwell experiments

To establish polarized pBCEC cultures, cells were plated onto collagen-coated (120 µg/ml) transwell (6- or 12-well) culture dishes at a density of 40,000 cells/cm^2. Cells were grown for 2–3 days depending on the transendothelial electrical resistance (TEER; 50 ohms/cm^2). The tightness of the transwell culture was assessed by measuring TEERs using an EndOhm tissue resistance measurement chamber and EndOhm ohmmeter (World Precision Instruments, Florida). TEERs of collagen-coated, cell-free filters were used as blanks. Tight junction formation was induced (overnight) by adding DMEM/Ham's F-12 medium containing 550 nM hydrocortisone, 1% penicillin/streptomycin, and 0.7 mM L-glutamine along with cholesterol [100 µM], simvastatin [5 µM], or vehicle only (EtOH, 0.5 %). Establishment of intact tight junctions was indicated by TEERs rising between 300 and 1000 ohms/cm2 in the in vitro BBB model system.

2.5. Animal studies

Animal studies were performed with ethical approval of the Austrian Department of Science, Research and Economy (approval number 66010/0052-WF/V/3b/2015). Female 3xTg AD mice and non-transgenic (Non-Tg) C57/Bl6 Mice were maintained in a 12-h light/ 12-h dark cycle in a temperature-controlled environment with free access to chow diet (Ssniff, Germany). Aged mice (Non-Tg: 58 ± 11 weeks, 3xTg AD: 64 ± 4 weeks) were gavaged for 21 days with vehicle only or 40 mg/kg simvastatin in 0.2% agarose in PBS. Blood samples were taken prior to treatments and upon sacrification. Plasma lipids were measured enzymatically using colorimetric assay kits (DiaSys Diagnostic Systems; Supplemental Fig.I).

2.6. Isolation of mBCEC

Mice were sacrificed and murine brain capillary endothelial cells (mBCEC) were isolated from a pool of 2 hemispheres (Non-Tg +/-sim: n=4; 3xTg +/-sim: n=8). In brief, hemispheres were washed in PBS (containing 2% penicillin/streptomycin) and the olfactory bulb was removed. Scalpel and douncer were used to mince the grey and the white matter of the cortex. To isolate the capillaries, the homogenate was mixed with dispase (0.01 g /2 hemispheres) in 5 ml MCDB131 medium (containing 2% FBS, 1% L-glutamine and 10% penicillin/streptomycin) and incubated at 37°C in the water bath for 1 h. Disruption of the capillaries followed by endothelial cell isolation using Percoll bi-phase gradient was performed as described above for pBCEC (48).

2.7. Isolation of plasma-derived apoJ

ApoJ was isolated from human plasma as described by Dabbs and Wilson (49). In brief, plasma was prepared by centrifuging human blood containing 10 mM sodium citrate. After addition of Complete® protease inhibitor, debris was removed with a GFC glass fibre filter (MicroAnalytic Products Inc., Mountain Lakes, NJ, USA) and a 0.45 µm cellulose nitrate filter. ApoJ was isolated from the plasma using a G7 anti-CLU monoclonal antibody column (50) connected to an Econo pump system (Biorad). ApoJ bound to the column was eluted using 2 M GdHCl in PBS and dialysed against 20 mM MES, pH 6.0. A 1 ml HiTrap™ SP XL cation exchange column (GE healtchcare) was used to collect apoJ from the dialysed fraction.

2.8. Lipid extraction and GC-MS analysis

For measuring brain cholesterol and precursors (Supplemental Fig.II), hemispheres of murine brains were subjected to lipid extraction according to the Folch method. Folch solution (chloroform/methanol, 2:1 (v/v)) was added and tissues homogenized using an Ultra-turrax T25 basic (IKA). After 2 h at room temperature, vials were centrifuged (840 g, 10 min), and extracts transferred to new vials, solvents evaporated under argon, and redissolved in appropriate volumes of Folch and stored at –20 °C until measurements.

For measuring cellular cholesterol precursors, pBCEC were cultured in 75 cm² flasks until confluent and incubated for 24 h in the absence or presence of 5 µM simvastatin in serum-free medium. For measuring cholesterol synthesis, pBCEC were incubated for 24h with simvastatin [5 µM] and vehicle control (0.5% ethanol) in the presence of 10% deuterium water (D_2O) in serum-free medium. Cellular lipids were extracted with Folch's solution (chloroform:methanol= 2:1 (v/v)) for 30 min at room temperature.

Cholesterol precursors and deuterium enrichment in newly synthesized cholesterol was determined using combined gas chromatography-mass spectrometry (GC-MS) analysis as described previously (51). In brief, after lipid extraction certain amounts of the extract were hydrolyzed in 1 M NaOH in ethanol and incubated in a water bath for 1 h at 65°C. Cyclohexane was used to extract the organic phase which then was evaporated and silylated by treating with pyridine/ hexamethyldisilazane/ chlorotrimethylesilane (3:2:1, v/v/v) at 60°C for 30 min. After evaporation of the solvent, hexane was added and then transferred into special glass vials. Cholesterol precursors were determined using deuterium-labeled internal standards (d6-cholesterol, d4-lathosterol and d6-sitosterol). GC-MS analysis was performed as described previously on a Hewlett Packard 6890 Series Plus gas chromatograph using a gas chromatograph column (52). Enrichment of deuterium in cellular cholesterol was calculated as described by Diraison et al. (53).

2.9. BACE Activity Assay

The activity of β-secretase BACE1 was examined using the Beta Secretase Activity Assay Kit from Abcam. In brief, pBCEC were treated with vehicle control (ethanol) or simvastatin [5μM] for 24 h followed by treatment with lysis buffer and subsequent determination of BACE activity using 100 μg of cellular protein. Activity was measured fluorescently using a fluorimeter (FlexStation II, Molecular Devices; Ex= 345 nm/Em: 500 nm).

2.10. Isolation of RNA and quantitative real-time PCR

pBCEC were grown in 12-well plates and incubated in serum-free M199 medium with vehicle control (0.5% ethanol), 24*(S)*-hydroxycholesterol [10 μM], 27-hydroxycholesterol [10μM], TO901317 [2μM], cholesterol [100 μM], simvastatin [5 μM], purified apoJ [2 μg/ml or 20 μg/ml], or increasing concentrations of soluble $A\beta_{(1-40)}$ [25 ng/ml, 50 ng/ml or 200 ng/ml]. In addition, pBCEC were incubated with a combination of plasma-derived apoJ [2μg/ml] and $A\beta_{(1-40)}$ [50 ng/ml] after a 30 min preincubation in serum-free M199 medium at 37℃. For cell culture experiments, simvastatin was activated prior to use according manufacturer's protocol (54). Cells from 3 wells were pooled and resuspended in 1 mL TriReagent RT (MRC, USA). For animal studies, RNA was isolated from cell lysates of mBCEC using 1ml TriReagent RT. Whole brain mouse tissue (~50 mg) was minced by adding 1 ml TriReagent RT and by using a tissue homogenizer (Ultra Turrax) for 3x10 seconds. To reach a phase separation, 50 μl 4-bromoanisole (BAN) was added, the suspension was incubated for 5 min at room temperature and centrifuged (12 000xg, 15 min, 4℃). The aqueous phase of the suspension was isolated and mixed with isopropanol 1:1 (v/v). After 10 min of incubation at room temperature and a centrifugation step (12 000xg, 8 min, 4℃), the pellet was washed once with 75% ethanol. The RNA pellet was air dried and resuspended in 40 μl RNase free water. To dissolve the RNA, the samples were incubated for 10 min in the thermocycler (55℃, 300 rpm) and the concentration and purity was determined using a Nanodrop. Relative gene expression levels were determined by reverse transcriptase (RT)-quantitative real-time PCR (qPCR) based on SYBR Green detection chemistry. For cDNA synthesis the "High Capacity Reverse Transcriptase Kit" by Life Technologies was used according to manufacturer's instructions. On average, 500 ng of RNA was reversed to receive a final concentration of 5 ng/μl of cDNA. Control reactions lacking reverse transcriptase were prepared in order to check for genomic DNA contamination. qPCR were prepared by using SYBR Green Master Mix (Biorad) according to the manufacturer's recommendations. In general, each reaction (10 μl) contained 1×iQ SYBR Green Supermix (Bio-Rad), 300 nmoles of each primer (Table 1), and 10 ng of cDNA template; PCR cycling conditions consisted of 40 cycles at 95 ℃ for 20 s, 60 ℃ for 40 s, and 72 ℃ for 40 s. All reactions were run in triplicates, and melting curve analyses were routinely performed to monitor the specificity of

the PCR product. Relative gene expression was quantified by using the *ΔΔCt* method described by Livak and Schmittgen (55).

2.11. RNA interference mediated apoJ silencing in pBCEC

A pool of 3 small interfering (si)RNA targeting apoJ mRNAs was purchased from Microsynth. At 50-60% confluency, pBCEC were transfected with 25 nM and 50 nM of the prepared mix of the 3 apoJ siRNAs (Table 2) using PrimeFect Diluent and PrimeFect Reagent as described by Stefulj *et al.* (56). Transfected cells were incubated for 28-30 h at 37°C. In parallel, silenced pBCEC were incubated with 5 µM simvastatin for 24 h, and/or 50 ng/µl $A\beta_{(1-40)}$ for additional 1 h in serum-free conditions. Scrambled siRNA was used as non-coding siRNA with minimal unintended off-target effects.

2.12. SDS-PAGE and immunoblotting

pBCEC were grown in 6-well plates and incubated with serum-free medium containing vehicle control (0.5 % ethanol), 24*(S)*-hydroxycholesterol [10 µM], 27-hydroxycholesterol [10µM], TO901317 [2µM], cholesterol [100 µM], simvastatin [5 µM], purified apoJ [2 µg/ml or 20 µg/ml], and/or increasing concentrations of soluble $A\beta_{(1-40)}$ [25 ng/ml, 50 ng/ml or 200 ng/ml]. Additionally, pBCEC were treated with a combination of plasma-derived apoJ [2µg/ml] and $A\beta_{(1-40)}$ [50 ng/ml] after 30min preincubation at 37°C. For cell culture experiments, simvastatin was activated prior to use according manufacturer's protocol (54). Intracellular and secreted proteins were isolated after an incubation period of 1 h and 24 h. To isolate secreted proteins, the medium was collected and centrifuged at 10 000xg for 10 min at 4°C. Proteins were precipitated by adding 3% (v/v) trichloroacetic acid (TCA), and incubation for 1 h on ice. The suspension was centrifuged (10 000xg, 10 min, 4°C), the pellet was washed twice with ice cold acetone, and dissolved in 1x sample buffer (Biorad) and 1x Reducing Agent (Biorad). After removing the medium from the 6-well plates, cells were washed twice with cold 1x PBS and lysed in protein lysis buffer (50 mm Tris, 10 mm EDTA, 1% Triton X-100, 0.5% v/v protease inhibitor mixture, pH 7.4). Cell lysates were vortexed, sonicated in a water bath sonicator for 2x3 min, and centrifuged (10 000xg, 10 min, 4°C) to remove residual DNA. Protein concentrations were measured by the BCA assay (Thermo Scientific) and 15 µg of the proteins (mixed with 1x loading buffer, 1x reducing agent) were loaded onto NuPage® Novex 4-12% Bis- Tris Midi Gels (Thermo Scientific) after proteins were denatured at 95°C for 5 min in a thermocyler. Proteins were separated by SDS-PAGE using the method described by Laemmli (57). Western blotting was performed according to Haid and Suissa (58) using 0.45 µm PVDF membranes (GE healthcare). After blocking with 5% non-fat dry milk (Biorad) in TBS-TT for 1 h the membrane was probed with rabbit polyclonal anti-APP antibody (Invitrogen; 1:1000), rabbit polyclonal A11 anti-amyloid oligomers antibody

(Millipore; 1:10 000), rabbit polyclonal anti-APP/CTF (Sigma, 1:4000), rabbit polyclonal anti-apoJ (Cloud-Clone Corp, 1:500; Santa Cruz Biotechnology, 1:500), goat anti- LRP1 1704 (1:10 000), mouse anti- LRP1 B411E2 (1:1000), or rabbit polyclonal anti-β-actin (Sigma; 1:5000) overnight at 4°C. After incubation of the blot with the adequate HRP-conjugated secondary antibody, signals were detected using Clarity Western ECL Substrate (Biorad) and exposure to x-ray films (Thermo Scientific). Films were scanned and bands densitometrically analyzed using Image J software (version 1.47v). Immunoblot analysis of mBCEC was performed using cell lysates of freshly isolated mBCEC without cultivation.

2.13. Aβ uptake studies

pBCEC were grown in collagen-coated 24-well plates until confluent and incubated with vehicle control (ethanol) or simvastatin [5 µM] for 24 h. Aβ uptake assay was performed by adding 0.3 nM of [^{125}I]-A$\beta_{(1-40)}$ and incubating at 37°C for 22 h. Alternatively, for examining uptake of A$\beta_{(1-40)}$ in combination to treatment with purified apoJ [2 µg/ml or 20 µg/ml], Alexa Fluor 488 (AF488) labelled A$\beta_{(1-40)}$ was used and pBCEC were incubated at 37°C for 3 h and 24 h. To allow complex formation apoJ was incubated with AF488-A$\beta_{(1-40)}$ at 37°C for 30 min prior to cell treatment. Cells were washed twice with ice-cold PBS and medium and PBS were collected and subjected to TCA precipitation (30%TCA). Cells were lysed by adding 0.3 N NaOH and subsequently subjected to protein precipitation with 100% TCA. Total cellular protein concentration was quantified using the Qubit fluorometer (Quant-IT protein assay kit, Invitrogen). Uptake of ^{125}I-A$\beta_{(1-40)}$ was calculated as the percentage of cpm/mg cell protein in the pellet of cell lysates relative to the pellet of supernatants. Uptake of AF488-A$\beta_{(1-40)}$ was determined using a fluorescent plate reader.

2.14. Aβ transport studies

pBCEC were grown on collagen coated [120 µg/ml] 12-well transwell filters, incubated in DMEM/Ham's F12 medium containing 1% P/S, 0.25% glutamine (Sigma Aldrich). Cells were grown for 2-3 days depending on the transendothelial electrical resistance (TEER). TEER was measured by using an EndOhm tissue resistance chamber and the Evohm ohmmeter (World Precision Instruments). Tight junction formation was induced (overnight) by adding 550 nM hydrocortisone to DMEM/Ham's F-12 medium containing 1% penicillin/streptomycin, and 0.7 mM L-glutamine. To test effects on A$\beta_{(1-40)}$ transport, pBCEC were incubated with 5 µM simvastatin prior to transcytosis experiment. In additional experiments, 2 µg/ml of apoJ was added to the basolateral compartment. Aβ transport assay was performed by adding 0.3 nM [^{125}I]-A$\beta_{(1-40)}$ and 100 nM [^{14}C]-sucrose as non-diffusion control to the basolateral compartment of transwell chambers. Transport of [^{125}I]-A$\beta_{(140)}$ from the basolateral/input ('brain parenchymal') to the apical/acceptor ('blood') compartment was studied during 2 h.

From each input and apical (acceptor) compartment, respectively, 400 µl and 50 µl were taken to examine transport of [^{125}I]-A$\beta_{(1-40)}$ and [^{14}C]-sucrose. [^{14}C]-sucrose was used as paracellular transport control which is not taken up by cells (59). To detect transport of intact [^{125}I]-A$\beta_{(1-40)}$, 400 µl aliquots of media were subjected to TCA precipitation and pellets were counted on a γ-counter. 50 µl of input and acceptor were counted on a β-counter with 5 ml Ultima Gold scintillation cocktail to examine passive diffusion of [^{14}C]-sucrose across the BBB. The transcytosis quotient (TQ) was calculated as followed:

$$\text{A}\beta\ \text{TQ} = \frac{\frac{[125\text{I}] - \text{A}\beta\ acceptor}{[125\text{I}] - \text{A}\beta\ input}}{\frac{[14C] - \text{sucrose}\ acceptor}{[14C] - \text{sucrose}\ input}}$$

2.15. Cytotoxicity assay

Cytotoxicity assay was performed using cell proliferation Reagent WST1 by Roche. In brief, pBCEC were plated onto collagen coated [60 µg/ml] 96 well plates. Upon reaching confluency, cells were treated for 24 h with increasing concentrations of A$\beta_{(1-40)}$ [25 ng/ml, 50 ng/ml, or 200 ng/ml]. Absorbance of the formazan product was measured using fluorimeter FlexStation II (Molecular Devices) at 450 nm when 650 nm was used as reference wavelength.

2.16. Single/double labeled immunofluorescence staining of pBCEC

Cerebrovascular endothelial cells were cultured on Lab-Tek chamber slides (Thermo Fisher Scientific, NY, USA) and were fixed with 4% paraformaldehyde (PFA) for 10 min. After fixation, cells were washed in TBST and blocked with donkey serum for 30 min before primary antibodies incubation for 1 h (rabbit anti-human Zo-1/ TJP1 1.0µg/ml (Thermo Fisher Scientific, IL, USA), mouse anti-human VE-cadherin (F-8) 0.4µg/ml) (Santa Cruz Biotechnology, Inc., TX, USA) and anti-rabbit Lrp1 (1704)- obtained from Prof. Claus Pietrzik. All incubation steps were performed in a dark moist chamber at room temperature. After 5 min of TBST wash, secondary antibodies were applied: donkey anti-rabbit Cy-3 (red) 2.0µg/ml (Jackson Immuno Lab, Inc., West Grove, PA, USA) and donkey anti-mouse Dylight 488 (green) 1.67µg/ml (Jackson Immuno Lab, Inc., West Grove, PA, USA) for 30 min. After rinsing in TBST, DAPI was added to the slides for 20 min as a nuclei counter stain. Sections were rinsed again with TBST before mounting with Vectashield mounting medium (Vector Lab, Inc., Burlingame, CA, USA). Normal rabbit immunoglobulin fraction (Millipore Corp., Temecular, Ca, USA) and mouse immunoglobulin fraction (CedarlaneLab, Burlington, NC, USA) were used as negative controls. To acquire and analyze computerized images of sections and cells, a Leica DM4000 B microscope (Leica Cambridge Ltd) equipped with Leica DFC 320 Video camera (Leica Cambridge Ltd) was used.

2.17. Statistics

Results are reported as mean±SD unless stated otherwise. All experiments were performed at least three or more times in triplicates. Statistical significances (*p<0.05: **p<0.01; ***p< 0.001) were determined by analysis of variance (ANOVA) or two-tailed Student's t-test performed with Prism software (*Graphpad version* 6, CA, USA).

3. RESULTS

3.1. Simvastatin stimulates expression and secretion of apoJ in cerebrovascular endothelial cells

To investigate regulatory effects of modulators of cholesterol metabolism on mRNA and protein levels of apoJ, pBCEC were incubated for 24 h with vehicle (0.5% ethanol), the natural LXR ligands 24*(S)*OH-cholesterol [10 µM] or 27OH-cholesterol [10 µM], the synthetic LXR ligand TO901317 [2 µM], the HMG-CoA reductase inhibitor simvastatin [5 µM], or cholesterol [100 µM] itself. Simvastatin induced a 2.1±0.43-fold increase in apoJ mRNA levels while neither cholesterol, nor LXR agonists exerted significant effects on apoJ mRNA or protein expression levels in pBCEC (Fig. 1A). To see whether effects of simvastatin treatment on apoJ levels are related to the altered cellular cholesterol status elicited by the statin or caused by other/pleiotropic effects, pBCEC were incubated in the presence or absence of simvastatin [5 µM], cholesterol [100 µM], or a combination of simvastatin [5 µM] and cholesterol [100 µM]. Immunoblotting revealed a 2.3±0.77-fold increase in apoJ protein expression by pBCEC in response to simvastatin (Fig. 1B). Neither cholesterol nor a combination of cholesterol and simvastatin changed cellular apoJ levels. This indicates that effects of simvastatin on apoJ levels are likely mediated by its inhibition of cellular cholesterol synthesis.

Since apoJ protein is known to be present in two forms (60), i.e. secreted (representing the more abundant form) or remaining within the cell, we examined levels of apoJ released by polarized pBCEC cultured on Transwell filters, to the apical (mimicking the blood-side of the BBB) and the basolateral (mimicking the brain parenchymal side of the BBB) compartment. Secretion of apoJ (during 24 h) to both the basolateral and apical compartments was observed, interestingly with a 3.2±0.58-fold higher amount of apoJ detected in the basolateral media (Fig. 1C). Furthermore, levels of apoJ in the basolateral compartment increased by 1.8±0.22-fold in response to simvastatin [5µM] treatment while cholesterol [100µM] treatment had no significant effects (Fig. 1D).

To confirm effects of 24 h simvastatin treatment on cholesterol synthesis in pBCEC, we performed GC-MS analysis from cell lipid extracts to measure deuterium isotopes incorporated into cholesterol molecules during incubation in the absence or presence of simvastatin in medium containing 10% deuterium water. We detected a 73.5±6.5% reduction in deuterium enrichment and hence a clear inhibition of cholesterol synthesis in response to treatment with 5 µM simvastatin (Fig. 1E). To confirm results, we additionally measured levels of cholesterol precursors (Fig. 1F). Here we found a reduction of desmosterol (72.4±3.58%), lathosterol (72.0±7.31%), lanosterol (81.2±2.37%), FF-MAS (85.1±9.81%) and T-MAS (69.6±4.16%) in response to simvastatin treatment.

3.2. Simvastatin influences APP expression and processing pathways in cerebrovascular endothelial cells

Beyond its original role in treating dyslipidemia it was shown that statin treatment reveal beneficial effects in progressive neurodegenerative diseases by reducing Aβ formation and burden (61). Therefore, we were interested to study the effects of cholesterol and simvastatin on mRNA and protein levels of APP, APP processing products, and APP processing enzymes in pBCEC (Fig. 2). We detected an increase by 78±24.7 % in relative APP mRNA levels in response to simvastatin treatment (5 µM, 24 h), which was accompanied by an equally increased (84±13.4 %) transcription of the non-amyloidogenic enzyme α-secretase (ADAM10) and reduced (53±28.7 %) transcription of the amyloidogenic enzyme BACE1 (β-secretase) (Fig. 2A). By contrast, cholesterol treatment (100 µM, 24 h) neither influenced APP, nor ADAM10 or BACE1 mRNA expression levels in pBCEC. In line with mRNA data, we detected a 2.1±0.60-fold increase in cellular protein levels of full-length APP (Fig. 2C) and a moderate (14±3.3%) decrease in BACE activity (Fig. 2B) in response to simvastatin treatment. The combined treatment with cholesterol [100 µM] and simvastatin [5 µM] diminished effects seen with simvastatin alone from 2.1±0.60-fold to 1.5±0.34-fold increase in cellular APP protein levels. In additional western blot experiments we detected a 3.4-fold increase in CTF (C-terminal fragments), APP cleavage products representing increased APP processing (Fig. 2D). No significant changes in CTF levels were observed when pBCEC were treated with either cholesterol or a combination of cholesterol and simvastatin, indicating that addition of cholesterol may reverse effects observed with simvastatin. In line with enhanced ADAM10 expression (Fig. 2A), simvastatin treatment increased levels of the secreted, beneficial APP cleavage product APPα (sAPPα) by 41±0.25% (Fig. 2E). Combined treatment with simvastatin and cholesterol also increased sAPPα protein levels, but to lower extent (33±0.19%) as compared to simvastatin alone, indicating that the effect of simvastatin is partly mediated through inhibition of cellular cholesterol synthesis. To sum up, we

conclude that simvastatin treatment shifts APP processing towards the beneficial, non-amyloidogenic pathway in cerebrovascular EC.

Further analysis of the amyloidogenic products formed from APP demonstrated a shift in cellular and secreted Aβ oligomer levels in response to treatment with simvastatin: relative protein amounts of cell-associated Aβ oligomers were significantly reduced (by 50±11.8%, Fig. 3A), whereas extracellular Aβ oligomers detected in the medium were increased (by 51±11.4%, Fig. 3B) as compared to control pBCEC. Aβ oligomers were detected in pBCEC using an amyloid oligomer specific antibody (A11), as described and characterized by Schweinzer *et al* (44). In addition, cellular uptake of [^{125}I]-A$\beta_{(1-40)}$ was reduced upon simvastatin treatment by 17±8.5% (Fig. 3C). In subsequent transcytosis experiments we examined the transport of ^{125}I labelled A$\beta_{(1-40)}$ from the basolateral (abluminal/brain parenchymal) to the apical (luminal/blood) compartment of pBCEC transwell cultures mimicking the BBB. Simvastatin exerted no significant effect on transport of exogenous A$\beta_{(1-40)}$ across the BBB (Fig. 3D).

These results taken together indicate that simvastatin treatment leads to reduced cellular load of cytotoxic Aβ oligomers in line with both reduced Aβ production and reduced cellular Aβ uptake by pBCEC, while clearance of Aβ across polarized cells is not compromised.

3.3. ApoJ regulates APP protein expression, Aβ formation, and clearance in pBCEC

To investigate potential effects of apoJ on APP expression and processing, apoJ was silenced using small interfering RNA. We observed a 54±2.2% and 54±1.9% reduction in apoJ mRNA levels using 25 nM and 50 nM of siRNA, respectively (
Fig. 4A), the latter yielding a more pronounced (by 56% as compared to 44%) reduction of cellular apoJ protein levels (
Fig. 4B). Thus all further studies were conducted using 50 nM of siRNA.

To examine the effects of apoJ silencing on proteins involved in the amyloid pathway, immunoblotting of APP, cellular and secreted Aβ oligomer levels was performed. Western blot analysis revealed a 56±19.8% reduction of intracellular APP protein levels (
Fig. 4C) and a reduction by 53±28.9% of intracellular Aβ oligomer levels (
Fig. 4D) in response to apoJ silencing. ApoJ silencing did not affect mRNA levels of APP, ADAM10, BACE1, or HMG-CoA-reductase (data not shown).

We next examined effects of exogenous apoJ on APP expression and processing in pBCEC. Porcine BCEC were incubated for 24 h in presence of 2 or 20 µg/ml of purified plasma apoJ (matching approximate concentrations detected in CSF and plasma, respectively (62). In line with the contrary results obtained during apoJ silencing experiments,

we detected a 3.3±1.19-fold and 2.4±0.20-fold higher amount of full-length APP protein in response to 2 µg/ml and 20 µg/ml apoJ treatment, respectively, while a combination of 20 µg/ml apoJ and 5 µM simvastatin increased protein levels of full-length APP up to 2.6±0.78-fold (Fig. 5A). On the other hand, we did not observe any significant changes in mRNA expression levels of genes involved in APP processing, nor HMGR, ABCA1 or SREBP2 in response to treatment with apoJ (Fig. 5B). Only the combined treatment with apoJ and simvastatin led to changes, confirming simvastatin as the major modifier. To examine the role of apoJ in Aβ transport across the BBB, pBCEC were grown on transwell filters, incubated for 2 h with 2 µg/ml exogenous apoJ added to both compartments, and transcytosis of radiolabelled Aβ peptides from the basolateral to the apical compartment was monitored. These experiments revealed that apoJ increases the transcytosis rate of [^{125}I]-A$\beta_{(1-40)}$ by 21±3.4% (Fig. 5C). In total a mean of 23.6±10.33% [^{125}I]-A$\beta_{(1-40)}$ was transported from the basolateral to the apical compartment, comparing to 4.6±2.80% transport of [^{14}C]-sucrose (Fig. 5D). Tightness of the endothelial barrier was assessed by measuring TEER values (Fig. 5E). TEER values rose from day 1 to day 2 after plating pBCEC on transwell filters from 96±9.2 to 142±18.6 ohm/cm². After induction of tight junction formation by addition of hydrocortisone [550 nM], TEER values increased by 2.3-fold reaching 332±24.1 ohm/cm². Treatment of pBCEC did not affect barrier tightness. Tight junction formation in pBCEC incubated in presence or absence of hydrocortisone [550 nM] was also examined by immunofluorescence microscopy (Fig. 5F). Tight junctions were visualized by anti-ZO-1 antibody and anti-VE-cadherin antibody. We observed a clear formation of tight junctions in pBCEC with and without induction with hydrocortisone. After incubation with hydrocortisone, pBCEC formed a more compact and organized barrier, as indicated also by TEER (Fig. 5E).

These results together strongly suggest an importance of apoJ in APP production and Aβ transport in cerebrovascular endothelial cells. As gene transcription analysis did not reveal significant changes upon modulation of apoJ levels in pBCEC, we hypothesized that the significance of apoJ is mainly based at the posttranslational level.

3.4. A$\beta_{(1-40)}$ affects apoJ expression and secretion in pBCEC

Having established that cellular apoJ levels as well as exogenous apoJ do modulate APP/Aβ processing and metabolism, we next studied potential alterations in apoJ expression and secretion caused by incubation of pBCEC in the presence of increasing (25, 50 and 200 ng/ml) concentrations of A$\beta_{(1-40)}$ for 1 h or 24 h. We used A$\beta_{(1-40)}$, since this is the most abundant amyloid peptide found in biological fluids and in cerebrovascular amyloid plaques (43). pBCEC were also treated with a combination of apoJ [2 µg/ml] and A$\beta_{(1-40)}$ [50 ng/ml].

mRNA expression analysis revealed an increase in apoJ mRNA levels by 37±9.7% and 35±13.9%, respectively, in response to 1 h incubation with 50 and 200 ng/ml $A\beta_{(1-40)}$ (Fig. 6A). Furthermore, a dose-dependent decrease in cellular apoJ protein expression was detected. Treatment with 25 ng/ml, 50 ng/ml, or 200 ng/ml $A\beta_{(1-40)}$ for 1 h led to reduction in cellular apoJ levels by 32±9.0%, 54±9.3% and 46±9.5%, respectively (Fig. 6C). In addition, the combined treatment with Aβ and apoJ decreased cellular apoJ protein levels by 65.6±10.6%. Treatment of pBCEC with $A\beta_{(1-40)}$ for 24 h resulted in a less pronounced, but still significant reduction in cellular apoJ protein levels (by 25±17% and 29±10.6% in response to 50 ng/ml and 200 ng/ml of $A\beta_{(1-40),}$ respectively; Fig. 6C, right side), and a dose-dependent increase in secreted apoJ protein levels (by 1.5±0.20-fold and 2.5±0.39-fold in response to 50 ng/ml and 200 ng/ml $A\beta_{(1-40),}$ respectively; Fig. 6B) These results together suggest us that enhanced transcription and secretion of apoJ in response to $A\beta_{(1-40)}$ may serve to counteract the Aβ challenge and protect the cells by scavenging extracellular $A\beta_{(1-40)}$.

In cell proliferation assays using WST1 reagent (Roche), no cytotoxic effects were observed for any of the concentrations of $A\beta_{(1-40)}$ used (Fig. 6D).

3.5. Effects of apoJ and $A\beta_{(1-40)}$ on receptors involved in Aβ clearance at the BBB

To test whether the addition of apoJ prevents Aβ from binding to pBCEC and subsequent uptake, we performed an uptake assay using fluorescently (Alexa Fluor 488) labelled $A\beta_{(1-40)}$. We found that a 3 h treatment with 2 and 20 µg/ml purified apoJ led to a dose-dependent reduction in uptake of Alexa Fluor488 labelled $A\beta_{(1-40)}$ by 40±17.6% and 59±11.0%, respectively (Fig. 7A). An incubation time of 24 h led to an even more significant reduction in the uptake by 28±9.3% and 64±10.6%, respectively, confirming our hypothesis.

To examine the importance and influence of receptors known to be involved in Aβ transport, pBCEC were incubated for 1 h with different concentrations of $A\beta_{(1-40)}$ or a combination of $A\beta_{(1-40)}$ and apoJ (Fig. 7B). Interestingly, we detected a dose-dependent increase in LRP1 mRNA levels in response to treatment with 25 ng/ml (1.5±0.28-fold), 50 ng/ml (1.9±0.25-fold), or 200 ng/ml (2.2±0.24-fold) $A\beta_{(1-40)}$ as compared to pBCEC incubated in the absence of Aβ peptides. Stunningly, the combined treatment with $A\beta_{(1-40)}$ [50 ng/ml] and apoJ [2 µg/ml], reduced LRP1 mRNA expression back to normal (untreated conditions), again in accordance with apoJ 'scavenging' extracellular Aβ. In addition, at the highest concentration used (200 ng/ml), $A\beta_{(1-40)}$ also up-regulated mRNA levels of RAGE, LRP2 and P-glycoprotein (PGP)/multidrug resistance protein 1 (MDR1) by 2.1±0.55-fold, 2.3±0.48-fold and 1.6±0.22-fold, respectively.

In order to examine the effects of $A\beta_{(1-40)}$ on LRP1 at the protein level, antibodies recognizing two different epitopes were used (Fig. 8). Antibody LRP1 (B411E2) recognizes the N-terminus of LRP1 (63) and therefore detects the non furin-cleaved pre-mature form of LRP1 (600 kDa) as well as LRP1 α-chain (515 kDa), whereas LRP1 (1704) binds to the C-terminus of LRP1 (64) and therefore recognizes the cytoplasmic domain of the membrane-bound receptor LRP. $A\beta_{(1-40)}$ treatment had no influence upon protein expression levels of the cytoplasmic domain of LRP1, whereas treatment with 50 ng/ml, 200 ng/ml, or a combination of Aβ and apoJ led to a reduction of LRP1 α-chain level by 39±3.1%, 29±11.4% and 48±8.6%, respectively. An extended incubation period for 24 h did not confirm a dose-dependent increase of LRP1 mRNA levels in response to $A\beta_{(1-40)}$ treatment (Fig. 8C). Along with reduced levels of LRP1 α-chain, we detected 1.6±0.20-fold and 2.4±0.92-fold higher levels of secreted, soluble LRP1 (sLRP1) in the supernatants in response to treatment with 50 ng/ml and 200 ng/ml $A\beta_{(1-40)}$, respectively, as compared to untreated pBCEC (Fig. 8D). Combined treatment with 50 ng/ml $A\beta_{(1-40)}$ and apoJ [2 µg/ml] revealed significant increases (by 3.1±1.08-fold) in sLRP1 protein expression levels.

In addition, mRNA levels of ADAM10 and BACE1, the two APP processing enzymes also known to cleave membrane bound LRP1 to yield soluble LRP1 (28,29), were significantly increased in response to treatment with $A\beta_{(1-40)}$ (Fig. 7C,D). Treatment with 50 ng/ml or 200 ng/ml $A\beta_{(1-40)}$ increased relative gene expression of ADAM10 by 62±24.2% and 76±30.0%, respectively. Relative mRNA levels of BACE1 increased by 34±12.2% and 64±18.9% in response to 50 ng/ml and 200 ng/ml $A\beta_{(1-40)}$, respectively.

In summary these results strongly suggest that exposure of porcine cerebrovascular endothelial cells to $A\beta_{(1-40)}$ induces release of LRP1 from the cell surface, potentially mediated by ADAM10 and/or BACE1 and that the observed differences in $A\beta_{(1-40)}$ transport in presence of apoJ are the result of an sLRP1-dependent mechanism.

In subsequent studies we were interested to examine the effect of simvastatin and exogenous apoJ [2 and 20 µg/ml] on receptors expressed at the BBB, especially on LRP1. We found that simvastatin led to an increase in mRNA expression of LRP1, RAGE and PGP by 1.4±0.18-fold, 2.8±0.61-fold and 1.5±0.20-fold respectively (Fig. 8E). During additional immunoblot analysis we focused on LRP1 and confirmed an increase in protein levels by 77±77.0% in response to simvastatin treatment (Fig. 8F). In response to 2 µg/ml and 20 µg/ml apoJ treatment we detected an increase in LRP1 protein levels by 47±36.2% and 54±55.0%, respectively. By immunofluorescent staining we could also observe higher expression of LRP1 in response to simvastatin treatment (Fig. 8G). Treatment with 20 µg/ml

apoJ led to an even more pronounced increase in LRP1 expression levels. Taken these data together, we conclude that both, simvastatin and treatment with apoJ induce levels of receptors expressed at the BBB, confirmed for LRP1 at the protein level.

3.6. Simvastatin upregulates expression of apoJ, APP, Lrp1, ADAM10 and BACE1 in apoJ silenced cerebrovascular endothelial cells

In order to examine the effects of simvastatin and Aβ treatment in apoJ silenced cerebrovascular endothelial cells, we performed si-RNA experiments in combination with simvastatin and Aβ(1-40) treatment in pBCEC. We detected significant apoJ silencing effects (Fig. 9A) up to 79% with all conditions tested. However, we apoJ silencing efficiency was reduced by simvastatin treatment (2.0±0.26-fold). Similarily, simvastatin increased apoJ gene expression by 2.3±0.26-fold in apoJ silenced pBCEC treated with 50 ng/ml Aβ(1-40). Relative gene expression levels of APP (Fig. 9B), ADAM10 (Fig. 9C), BACE1 (Fig. 9D), and CTF protein levels (Fig. 9E) were significantly increased in response to simvastatin treatment in apoJ silcenced cells, regardless whether cells were coincubated with Aβ(1-40). Treatment with Aβ(1-40), on the other hand, did not reveal significant changes on APP, LRP1, ADAM10 or BACE1 mRNA expression nor CTF levels in apoJ silenced pBCEC. Although these results alltogether have to be interpreted with caution since simvastatin treatment appeared to inhibit silencing efficiency for apoJ, they suggest that simvastatin effects are maintained (with the exception of BACE1) under apoJ-silenced conditions in pBCEC.

3.7. Simvastatin affects APP processing and apoJ protein expression in 3xTg AD mice

In order to investigate *in vivo* effects of simvastatin on APP processing and apoJ expression at the BBB in a whole animal model, 3xTg AD and Non-Tg mice were gavaged with or without 40 mg/kg simvastatin in 0.2% agarose in PBS for 21 days. 3xTg AD mice are characterized by an overexpression of APP, presinilin1 and MAPT (microtubule associated protein tau) (65) and are prone to cerebrovascular/BBB dysfunction (66,67). In whole brain RNA of these animals we found a 2.5±1.10-fold increase in APP mRNA levels compared to Non-Tg mice (Fig. 10A). Moreover, we detected a clear 4.1±0.77-fold increase in Aβ oligomer levels in mBCEC isolated from 3xTg AD mice as compared to Non-Tg controls (Fig. 10B). Protein levels of the C-terminal fragments (CTF) - cleavage products of APP - revealed a 1.7-fold increase in 3xTg AD compared to Non-Tg mice, whereas simvastatin led to reduction in CTF levels by 50% in these mice indicating decreased APP processing in response to simvastatin (Fig. 10C). Simvastatin increased protein levels of apoJ in mBCEC of Non-Tg mice by 42% (Fig. 10D). Also, we found 2.5-fold higher apoJ protein levels in 3xTg AD mice compared to Non-Tg control mice. To further examine the role of receptors

expressed in endothelial cells in *in vivo* studies, RT-qPCR of mBCEC from 3xTg AD mice and Non-Tg control was performed. We found a 3.5±0.54-fold higher gene expression level of LRP1 in simvastatin treated 3xTg AD mice compared to Non-Tg controls (Fig. 10E). Further, treatment with 40 mg/kg simvastatin by oral gavage for 3 weeks increased LRP1 gene expression in 3xTg animals by 2.4±0.54-fold. In addition, mRNA levels of LRP2 of mBCEC from simvastatin treated 3xTg AD mice were increased up to 3.5±0.55-fold as compared to Non-tg animals and 2.4±0.54-fold relative to vehicle control treated 3xTg AD mice, whereas the expression profile of RAGE revealed unchanged.

4. DISCUSSION

In this study we demonstrate pronounced effects of the HMGCo-A reductase inhibitor simvastatin in primary brain capillary endothelial cells (BCEC) indicating a close interplay of cellular cholesterol metabolism, apoJ expression/secretion and Aβ production, metabolism, and clearance at the blood-brain interface.

Primary porcine brain capillary endothelial cells (pBCEC) were used as an *in vitro* model for our studies. These cells were shown to be actively involved in HDL biogenesis and Aβ processing at the blood-brain interface (44,68). Several studies have stated a correlation between cholesterol homeostasis in the brain, which seems to be isolated from that in the periphery, and Aβ metabolism (43,44,68). It is suggested that increasing cholesterol levels increase Aβ abundance. HDL, on the other hand was shown to have a protective role in neuroinflammation, oxidative stress and also in Aβ metabolism (69,70). It was demonstrated that HDL-like particles in the brain can bind to Aβ peptides and facilitate its clearance across the BBB (69,71). Furthermore, AD patients reveal significantly higher LDL cholesterol and significantly reduced HDL cholesterol (72). They were also reported to have higher apoJ expression levels, in particular present in neuritic plaques and cerebrovascular deposits (36). ApoJ reveals, in addition to its rather minor function in lipid trafficking, chaperone function, where it is involved in Aβ binding and transport (43). It was reported that apoJ is able to bind soluble Aβ with high affinity, especially monomeric $A\beta_{(1-40)}$, rather than Aβ aggregates (73). Furthermore, apoJ is fully functional to interact with Aβ when it is associated with HDL (74). Therefore, higher apoJ levels might be a marker of prevalent dementia but are not linked with risk of future dementia (75). Since more than 80% of AD patients also establish amyloid deposition in cerebral vessels (6), and cerebrovascular dysfunction was reported in 3xTg AD mice (66,67), we used this AD model in addition to non-transgenic animals for *in vivo* studies.

To examine the correlation of HDL biogenesis and apoJ, in initial *in vitro* experiments we determined whether regulators of the cellular cholesterol metabolism, such as the natural

LXR agonist 24*(S)*-hydroxycholesterol, 27-hydroxycholeseterol, the synthetic LXR agonist TO901317, cholesterol, or simvastatin - an inhibitor of HMGCo-A reductase and thus of cholesterol biosynthesis - influences apoJ expression in pBCEC. Only simvastatin markedly increased apoJ mRNA and cellular protein levels, whereas a combination of simvastatin and cholesterol did not change apoJ protein levels (Fig. 1A, B). This indicates that the cholesterol reducing effects of statin treatment causes observed change in apoJ levels, rather than cholesterol-independent "pleiotropic" effects. Preliminary results suggest that – in contrast to apoJ - simvastatin does not alter apoA-I expression in pBCEC, whereas apoE is not expressed at all in pBCEC (unpublished observations). In transwell studies we observed significantly higher secretion of apoJ towards the basolateral compartment when pBCEC were treated with simvastatin (Fig. 1D). During *in vivo* studies we detected higher apoJ protein levels in cerebrovascular endothelial cells isolated from 3xTg AD mice as compared to Non-Tg mice (Fig. 10D). Interestingly, patients suffering CAA also reveal a higher apoJ plasma profile (42). In addition and in accordance with our *in vitro* results, administration of simvastatin for 21 d increased apoJ levels in mBCEC isolated from Non-Tg mice. Our data indicate that simvastatin, a well-known inhibitor of cellular cholesterol synthesis, has the potential to enhance apoJ synthesis and secretion pathways in cerebrovascular endothelial cells.

In transwell experiments we determined polarized secretion of apoJ to the basolateral and apical compartment of the pBCEC monolayer. We detected predominant secretion of apoJ to the basolateral side (Fig. 1C). Also apoA-I is primarily secreted towards the brain compartment of the pBCEC monolayer and ABCA1 is localized at the basolateral membrane of pBCEC (68). Recently we reported that PLTP, another key protein involved in HDL biogenesis and remodelling, is mainly secreted towards the brain parenchymal side of the BBB (48), and our previous findings revealed that sAPPα (the beneficial cleavage product of APP) is also highly secreted to the basolateral side (44) of the BBB model. Thus, the brain parenchymal side of the BBB represents an important area for amyloid and cholesterol metabolism.

When examining effects of reduced cellular cholesterol synthesis in BCEC on APP processing, we observed increased APP mRNA and protein, increased secretion levels of the beneficial cleavage product sAPPα and ADAM10 mRNA expression in response to 5 µM simvastatin treatment, whereas relative gene expression as well as activity of the Aβ peptide forming β-secretase (BACE1) was decreased (Fig. 2B). A simultaneous treatment with cholesterol and simvastatin reduced APP and CTF levels, and therefore APP expression and processing as compared to solely simvastatin treatment (Fig. 2C,D). Hence, we conclude

that also here effects seen with simvastatin are caused by depletion of cellular cholesterol by simvastatin. Barrett *et al.* identified a cholesterol-binding domain within the APP transmembrane domain (76). Due to the fact that the cholesterol-binding site is immediately adjacent to the α-secretase cleaving site, it is hypothesized that binding of cholesterol may drive APP processing towards the amyloidogenic pathway. A reduction and redistribution of cellular cholesterol pools could account for this effect observed in statin treated pBCEC. Also, dysregulation of cholesterol trafficking was reported to interfere with APP metabolism since α-/β-secretase processing occurs within cholesterol rich lipid rafts in the membrane (77,78). Therefore, cholesterol depletion decreases membrane fluidity and thus leads to enhanced α-secretase activity (79). Taking these findings together with the fact that lower cellular cholesterol synthesis due to simvastatin treatment enhances gene expression of APP and α-secretase ADAM10 as well as sAPPα production, we conclude that simvastatin helps to direct APP towards the neuroprotective, non-amyloidogenic APP processing pathway in cerebrovascular EC. We earlier reported on modulation of cellular cholesterol synthesis by simvastatin and effects on APP production and processing at the blood-brain interface *in vitro* (44). Also in neurons activities of α- and β secretases display a dependency on membrane cholesterol contents (80). Simons *et al.*, for instance, reported that in cultured hippocampal neurons cholesterol depletion in response to combined treatment with lovastatin and methyl β-cyclodextrin inhibited Aβ production (81). Moreover, Cordy *et al.* demonstrated that Aβ generation in a neuronal cell line depends on lipid rafts. Changes in cholesterol and lipid distribution within cell membranes, which take place during aging, lead to higher concentrations of BACE and other amyloidogenic enzymes in lipid rafts and therefore more Aβ is produced (82). In addition, several studies reported that statin treatment decreased Aβ loads in animal models (21,83). When we performed *in vivo* studies, we found decreased production of both CTFα and β in cerebrovascular cells isolated from 3xTg AD mice in response to treatment with simvastatin (Fig. 10C). This indicates reduced APP processing and thus potentially reduced Aβ production in mBCEC.

Upon simvastatin treatment cell-associated oligomers are reduced in pBCEC, which may be beneficial for the cell - concomitantly, however oligomers/Aβ in the supernatants are increased. Depending on the fate of these oligomers, it is important to note that they may add an amyloidogenic component to simvastatin's effects to surrounding cells. We also studied uptake and transport of $A\beta_{(1-40)}$ in cerebrovascular endothelial cells. Uptake of [^{125}I]-labelled $A\beta_{(1-40)}$ in pBCEC was reduced in response to simvastatin treatment (Fig. 3). We conclude that reduced cellular cholesterol synthesis leads to a reduced Aβ uptake. Many receptors at the BBB are involved in the uptake of amyloid fragments, with LRP1 reported as the most important receptor to clear amyloid peptides from the brain and efflux them to the

plasma (84). By immunoblot analysis and immunofluorescence microscopy we demonstrate that simvastatin treatment increases LRP1 protein levels in pBCEC (Fig. 8F, G). In addition, we observed that $A\beta_{(1-40)}$ increased mRNA expression of RAGE, PGP, LRP2, but most pronouncedly of LRP1 in pBCEC (Fig. 7B). Also, gene expression of LRP1 and LRP2, but not of RAGE, was shown to be higher in mBCEC of simvastatin treated 3xTg AD mice compared to Non-Tg control animals (Fig. 10E). In western blot analysis we observed a reduction of LRP1 α-chain, whereas the cytoplasmic domain remained unchanged in response to $A\beta_{(1-40)}$ treatment (Fig. 8). Western blots performed with secreted proteins showed an increase in soluble LRP1 in response to 1 h treatment with $A\beta_{(1-40)}$. In further experiments we found that gene expression of both, BACE1 and ADAM10 was increased in response to $A\beta_{(1-40)}$ treatment (Fig. 7C,D). It was reported that α-secretase ADAM10, which belongs to the group of metalloproteinases, and β-secretase BACE1 are responsible for LRP1 shedding, which results in the production of sLRP1 (28,29). Surprisingly, we found that the combined treatment of $A\beta_{(1-40)}$ and apoJ did not enhance expression of LRP and other receptors at the BBB, whereas treatment with just 20 µg/ml apoJ increased the LRP1 β-chain in both, western blot analysis and with immunofluorescence microscopy (Fig. 8F,G). As we found reduced uptake of $A\beta_{(1-40)}$ in the presence of apoJ (Fig. 7A), we hypothesize that apoJ binds and scavenges Aβ in the extracellular space and thereby uptake and toxicity is reduced in pBCEC. In addition, we observed primarily enhanced secretion of LRP1 to the medium in response to additional treatment with $A\beta_{(1-40)}$. Therefore, we postulate that in pBCEC clearance/uptake of Aβ is activated through other mechanisms/receptors rather than membrane bound LRP1. Future studies will address this question.

In a series of experiments, we examined the effects of exogenous, purified plasma apoJ treatment as well as of apoJ silencing on mRNA and protein expression levels of genes involved in amyloid and cholesterol metabolism. During silencing studies, we observed that a reduction of apoJ using small interfering RNA lead to decreased full-length APP protein (Fig. 4C). Treatment with exogenous apoJ [2 µg/ml and 20 µg/ml], on the other hand, significantly increased APP protein levels (Fig. 5A). Therefore, we postulate a close connection and an important role of apoJ in APP metabolism in the cerebrovasculature.

When further elucidating the effects of amyloid peptides and apoJ expression and secretion, we found that $A\beta_{(1-40)}$ increased apoJ mRNA and secreted protein levels, whereas cellular apoJ levels were reduced after 1 h treatment and to a lesser extent after 24 h treatment (Fig. 6). As it was shown that apoJ tends to colocalize with amyloid plaques (85) and may avidly bind to Aβ (86), the observed data suggest that upon treatment with Aβ more apoJ is translated and secreted to the extracellular space to bind to $A\beta_{(1-40)}$ peptides. In contrast, it was reported by Wang *et al.* that treatment with $A\beta_{42}$ led to overexpression of

intracellular apoJ, but levels of secreted apoJ remained unchanged in primary hippocampal neurons (87). This indicates, that apoJ is regulated differently in different brain cell types in response to Aβ treatment. Zlokovic *et al.* and Merino-Zamorano *et al.* reported, however, that apoJ can facilitate Aβ clearance across well-established *in vitro* BBB models (43,88). In transport studies we observed increased clearance of [^{125}I]-labelled $A\beta_{(1-40)}$ from the basolateral to the apical side in the presence of apoJ, whereas overall cellular uptake was reduced (Fig. 5C, Fig. 7A). This is in accordance with the studies performed by Cole *et al.*, who reported that apoJ blocks binding, uptake and degradation of $A\beta_{42}$ in rat microglia (89). In other studies it was shown that apoJ reduced uptake of Aβ oligomers and fibrils in primary human adult microglia (90). In primary human astrocytes, on the other hand, just uptake of Aβ oligomers was impaired, whereas Aβ fibrils uptake remained unchanged (90).

As the function of apoJ in amyloid metabolism is quite controversial we were aiming to elucidate the mechanism of this chaperone in correlation with cholesterol metabolism in APP processing at the BBB. We clearly demonstrate that simvastatin treatment, which blocks cellular cholesterol synthesis, increases expression of APP and the α-secretase ADAM10, reduces the β-secretase BACE1 and hence, shifting APP processing towards the non-amyloidogenic pathway in cerebrovascular endothelial cells (Fig. 11). Moreover, due to simvastatin induced cholesterol depletion cellular Aβ uptake is decreased, leaving secreted Aβ increased. Our findings suggest a predominant secretion of apoJ from cerebrovascular endothelial cells to the brain parenchymal (basolateral) site of the BBB, where it can bind to Aβ and also helps in amyloid clearance across the BBB. Experiments showing increased secretion of apoJ to the extracellular space in response to treatment with soluble $A\beta_{(1-40)}$ also confirm this conclusion. Moreover, we clearly demonstrated that simvastatin and therefore reduced cellular cholesterol synthesis can regulate apoJ expression in brain endothelial cells both *in vitro* and *in vivo*. Results obtained from *in vitro* studies indicate a strong correlation of apoJ and APP protein levels. Addition of exogenous apoJ increased APP, whereas apoJ silencing reduced full-length APP and also cellular Aβ levels. Furthermore, we found that the presence of Aβ favorably leads to the secretion of the usually membrane bound receptor LRP1 in porcine cerebrovascular endothelial cells.

5. CONCLUSION

To sum up we suggest a close connection of statin treatment, apoJ and amyloid processing at the blood-brain interface. Future *in vivo* studies are aiming to elucidate and understand these mechanisms at the BBB in greater detail.

Acknowledgement: This work was supported by the Austrian Science Fund, grants P24783-B19 (to U.P.) and DK-MCD W1226-B18 (to U. P.), by the Medical University of Graz (Doctoral College of Metabolic and Cardiovascular Disease).

Conflict of interest: The authors declare that they have no conflicts of interest with the contents of this article.

REFERENCES

1. Burns A, Byrne EJ, Maurer K. Alzheimer's disease. Lancet. 2002 Jul 13;360(9327):163–5.

2. Wilquet V, De Strooper B. Amyloid-beta precursor protein processing in neurodegeneration. Curr Opin Neurobiol. 2004 Oct;14(5):582–8.

3. Zhang Y, Thompson R, Zhang H, Xu H. APP processing in Alzheimer's disease. Mol Brain. 2011;4:3.

4. Stukas S, Robert J, Wellington CL. High-Density Lipoproteins and Cerebrovascular Integrity in Alzheimer's Disease. Cell Metab. 2014 Apr 1;19(4):574–91.

5. Jellinger KA, Attems J. Prevalence and pathogenic role of cerebrovascular lesions in Alzheimer disease. J Neurol Sci. 2005 Mar 15;229–230:37–41.

6. Ghiso J, Fossati S, Rostagno A. Amyloidosis associated with cerebral amyloid angiopathy: cell signaling pathways elicited in cerebral endothelial cells. J Alzheimers Dis JAD. 2014;42 Suppl 3:S167-176.

7. Agyare EK, Leonard SR, Curran GL, Yu CC, Lowe VJ, Paravastu AK, et al. Traffic jam at the blood-brain barrier promotes greater accumulation of Alzheimer's disease amyloid-β proteins in the cerebral vasculature. Mol Pharm. 2013 May 6;10(5):1557–65.

8. Salminen A, Kauppinen A, Kaarniranta K. Hypoxia/ischemia activate processing of Amyloid Precursor Protein: impact of vascular dysfunction in the pathogenesis of Alzheimer's disease. J Neurochem. 2017 Feb;140(4):536–49.

9. Hardy J, Selkoe DJ. The amyloid hypothesis of Alzheimer's disease: progress and problems on the road to therapeutics. Science. 2002 Jul 19;297(5580):353–6.

10. Pera M, Alcolea D, Sánchez-Valle R, Guardia-Laguarta C, Colom-Cadena M, Badiola N, et al. Distinct patterns of APP processing in the CNS in autosomal-dominant and sporadic Alzheimer disease. Acta Neuropathol (Berl). 2013 Feb;125(2):201–13.

11. Martins IJ, Berger T, Sharman MJ, Verdile G, Fuller SJ, Martins RN. Cholesterol metabolism and transport in the pathogenesis of Alzheimer's disease. J Neurochem. 2009 Dec;111(6):1275–308.

12. Wood WG, Li L, Müller WE, Eckert GP. Cholesterol as a causative factor in Alzheimer's disease: a debatable hypothesis. J Neurochem. 2014 May;129(4):559–72.

13. Merched A, Xia Y, Visvikis S, Serot JM, Siest G. Decreased high-density lipoprotein cholesterol and serum apolipoprotein AI concentrations are highly correlated with the severity of Alzheimer's disease. Neurobiol Aging. 2000 Feb;21(1):27–30.

14. Bates KA, Sohrabi HR, Rainey-Smith SR, Weinborn M, Bucks RS, Rodrigues M, et al. Serum high-density lipoprotein is associated with better cognitive function in a cross-sectional study of aging women. Int J Neurosci. 2017 Mar;127(3):243–52.

15. Zhang J, Liu Q. Cholesterol metabolism and homeostasis in the brain. Protein Cell. 2015 Apr;6(4):254–64.

16. DeKosky ST. Statin therapy in the treatment of Alzheimer disease: what is the rationale? Am J Med. 2005 Dec;118 Suppl 12A:48–53.

17. Thelen KM, Rentsch KM, Gutteck U, Heverin M, Olin M, Andersson U, et al. Brain cholesterol synthesis in mice is affected by high dose of simvastatin but not of pravastatin. J Pharmacol Exp Ther. 2006 Mar;316(3):1146–52.

18. Papadopoulos P, Tong X-K, Hamel E. Selective benefits of simvastatin in bitransgenic APPSwe,Ind/TGF-β1 mice. Neurobiol Aging. 2014 Jan;35(1):203–12.

19. Tong X-K, Nicolakakis N, Fernandes P, Ongali B, Brouillette J, Quirion R, et al. Simvastatin improves cerebrovascular function and counters soluble amyloid-beta, inflammation and oxidative stress in aged APP mice. Neurobiol Dis. 2009 Sep;35(3):406–14.

20. Gibson Wood W, Eckert GP, Igbavboa U, Müller WE. Amyloid beta-protein interactions with membranes and cholesterol: causes or casualties of Alzheimer's disease. Biochim Biophys Acta. 2003 Mar 10;1610(2):281–90.

21. Fassbender K, Simons M, Bergmann C, Stroick M, Lutjohann D, Keller P, et al. Simvastatin strongly reduces levels of Alzheimer's disease beta -amyloid peptides Abeta 42 and Abeta 40 in vitro and in vivo. Proc Natl Acad Sci U S A. 2001 May 8;98(10):5856–61.

22. Pallebage-Gamarallage M, Takechi R, Lam V, Elahy M, Mamo J. Pharmacological modulation of dietary lipid-induced cerebral capillary dysfunction: Considerations for reducing risk for Alzheimer's disease. Crit Rev Clin Lab Sci. 2015 Dec 18;1–18.

23. Tarasoff-Conway JM, Carare RO, Osorio RS, Glodzik L, Butler T, Fieremans E, et al. Clearance systems in the brain-implications for Alzheimer disease. Nat Rev Neurol. 2015 Aug;11(8):457–70.

24. McIntee FL, Giannoni P, Blais S, Sommer G, Neubert TA, Rostagno A, et al. In vivo Differential Brain Clearance and Catabolism of Monomeric and Oligomeric Alzheimer's Aβ protein. Front Aging Neurosci. 2016;8:223.

25. Sagare AP, Deane R, Zlokovic BV. Low-density lipoprotein receptor-related protein 1: a physiological Aβ homeostatic mechanism with multiple therapeutic opportunities. Pharmacol Ther. 2012 Oct;136(1):94–105.

26. Pflanzner T, Janko MC, André-Dohmen B, Reuss S, Weggen S, Roebroek AJM, et al. LRP1 mediates bidirectional transcytosis of amyloid-β across the blood-brain barrier. Neurobiol Aging. 2011 Dec;32(12):2323.e1-11.

27. Herz J, Strickland DK. LRP: a multifunctional scavenger and signaling receptor. J Clin Invest. 2001 Sep;108(6):779–84.

28. von Arnim CAF, Kinoshita A, Peltan ID, Tangredi MM, Herl L, Lee BM, et al. The low density lipoprotein receptor-related protein (LRP) is a novel beta-secretase (BACE1) substrate. J Biol Chem. 2005 May 6;280(18):17777–85.

29. Liu Q, Zhang J, Tran H, Verbeek MM, Reiss K, Estus S, et al. LRP1 shedding in human brain: roles of ADAM10 and ADAM17. Mol Neurodegener. 2009;4:17.

30. de Gonzalo-Calvo D, Cenarro A, Martínez-Bujidos M, Badimon L, Bayes-Genis A, Ordonez-Llanos J, et al. Circulating soluble low-density lipoprotein receptor-related protein 1 (sLRP1) concentration is associated with hypercholesterolemia: A new potential biomarker for atherosclerosis. Int J Cardiol. 2015 Dec 15;201:20–9.

31. Bassett CN, Montine KS, Neely MD, Swift LL, Montine TJ. Cerebrospinal fluid lipoproteins in Alzheimer's disease. Microsc Res Tech. 2000 Aug 15;50(4):282–6.

32. Ladu MJ, Reardon C, Van Eldik L, Fagan AM, Bu G, Holtzman D, et al. Lipoproteins in the central nervous system. Ann N Y Acad Sci. 2000 Apr;903:167–75.

33. Maulik M, Westaway D, Jhamandas JH, Kar S. Role of cholesterol in APP metabolism and its significance in Alzheimer's disease pathogenesis. Mol Neurobiol. 2013 Feb;47(1):37–63.

34. Liu C-C, Liu C-C, Kanekiyo T, Xu H, Bu G. Apolipoprotein E and Alzheimer disease: risk, mechanisms and therapy. Nat Rev Neurol. 2013;9(2):106–18.

35. Lefterov I, Fitz NF, Cronican AA, Fogg A, Lefterov P, Kodali R, et al. Apolipoprotein A-I deficiency increases cerebral amyloid angiopathy and cognitive deficits in APP/PS1DeltaE9 mice. J Biol Chem. 2010 Nov 19;285(47):36945–57.

36. Nuutinen T, Suuronen T, Kauppinen A, Salminen A. Clusterin: a forgotten player in Alzheimer's disease. Brain Res Rev. 2009 Oct;61(2):89–104.

37. Fritz IB, Burdzy K, Sétchell B, Blaschuk O. Ram rete testis fluid contains a protein (clusterin) which influences cell-cell interactions in vitro. Biol Reprod. 1983 Jun;28(5):1173–88.

38. Humphreys DT, Carver JA, Easterbrook-Smith SB, Wilson MR. Clusterin has chaperone-like activity similar to that of small heat shock proteins. J Biol Chem. 1999 Mar 12;274(11):6875–81.

39. Li X, Ma Y, Wei X, Li Y, Wu H, Zhuang J, et al. Clusterin in Alzheimer's disease: a player in the biological behavior of amyloid-beta. Neurosci Bull. 2014 Feb;30(1):162–8.

40. Harold D, Abraham R, Hollingworth P, Sims R, Gerrish A, Hamshere ML, et al. Genome-wide association study identifies variants at CLU and PICALM associated with Alzheimer's disease. Nat Genet. 2009 Oct;41(10):1088–93.

41. Lambert J-C, Heath S, Even G, Campion D, Sleegers K, Hiltunen M, et al. Genome-wide association study identifies variants at CLU and CR1 associated with Alzheimer's disease. Nat Genet. 2009 Oct;41(10):1094–9.

42. Montañola A, de Retana SF, López-Rueda A, Merino-Zamorano C, Penalba A, Fernández-Álvarez P, et al. ApoA1, ApoJ and ApoE Plasma Levels and Genotype Frequencies in Cerebral Amyloid Angiopathy. Neuromolecular Med. 2015 Dec 14;

43. Zlokovic BV, Martel CL, Matsubara E, McComb JG, Zheng G, McCluskey RT, et al. Glycoprotein 330/megalin: probable role in receptor-mediated transport of apolipoprotein J alone and in a complex with Alzheimer disease amyloid beta at the blood-brain and blood-cerebrospinal fluid barriers. Proc Natl Acad Sci U S A. 1996 Apr 30;93(9):4229–34.

44. Schweinzer C, Kober A, Lang I, Etschmaier K, Scholler M, Kresse A, et al. Processing of endogenous AβPP in blood-brain barrier endothelial cells is modulated by liver-X receptor agonists and altered cellular cholesterol homeostasis. J Alzheimers Dis JAD. 2011;27(2):341–60.

45. Franke H, Galla H, Beuckmann CT. Primary cultures of brain microvessel endothelial cells: a valid and flexible model to study drug transport through the blood-brain barrier in vitro. Brain Res Brain Res Protoc. 2000 Jul;5(3):248–56.

46. Todd PA, Goa KL. Simvastatin. A review of its pharmacological properties and therapeutic potential in hypercholesterolaemia. Drugs. 1990 Oct;40(4):583–607.

47. Gerson RJ, MacDonald JS, Alberts AW, Kornbrust DJ, Majka JA, Stubbs RJ, et al. Animal safety and toxicology of simvastatin and related hydroxy-methylglutaryl-coenzyme A reductase inhibitors. Am J Med. 1989 Oct 16;87(4A):28S–38S.

48. Chirackal Manavalan AP, Kober A, Metso J, Lang I, Becker T, Hasslitzer K, et al. Phospholipid transfer protein is expressed in cerebrovascular endothelial cells and involved in high density lipoprotein biogenesis and remodeling at the blood-brain barrier. J Biol Chem. 2014 Feb 21;289(8):4683–98.

49. Dabbs RA, Wilson MR. Expression and purification of chaperone-active recombinant clusterin. PloS One. 2014;9(1):e86989.

50. Wilson MR, Easterbrook-Smith SB. Clusterin is a secreted mammalian chaperone. Trends Biochem Sci. 2000 Mar;25(3):95–8.

51. Saeed AA, Genové G, Li T, Lütjohann D, Olin M, Mast N, et al. Effects of a Disrupted Blood-Brain Barrier on Cholesterol Homeostasis in the Brain. J Biol Chem. 2014 Jun 26;289(34):23712–22.

52. Acimovic J, Lövgren-Sandblom A, Monostory K, Rozman D, Golicnik M, Lutjohann D, et al. Combined gas chromatographic/mass spectrometric analysis of cholesterol precursors and plant sterols in cultured cells. J Chromatogr B Analyt Technol Biomed Life Sci. 2009 Jul 15;877(22):2081–6.

53. Diraison F, Pachiaudi C, Beylot M. In vivo measurement of plasma cholesterol and fatty acid synthesis with deuterated water: determination of the average number of deuterium atoms incorporated. Metabolism. 1996 Jul;45(7):817–21.

54. Sadeghi MM, Collinge M, Pardi R, Bender JR. Simvastatin modulates cytokine-mediated endothelial cell adhesion molecule induction: involvement of an inhibitory G protein. J Immunol Baltim Md 1950. 2000 Sep 1;165(5):2712–8.

55. Livak KJ, Schmittgen TD. Analysis of relative gene expression data using real-time quantitative PCR and the 2(-Delta Delta C(T)) Method. Methods San Diego Calif. 2001 Dec;25(4):402–8.

56. Stefulj J, Panzenboeck U, Becker T, Hirschmugl B, Schweinzer C, Lang I, et al. Human endothelial cells of the placental barrier efficiently deliver cholesterol to the fetal circulation via ABCA1 and ABCG1. Circ Res. 2009 Mar 13;104(5):600–8.

57. Laemmli UK. Cleavage of structural proteins during the assembly of the head of bacteriophage T4. Nature. 1970 Aug 15;227(5259):680–5.

58. Haid A, Suissa M. Immunochemical identification of membrane proteins after sodium dodecyl sulfate-polyacrylamide gel electrophoresis. Methods Enzymol. 1983;96:192–205.

59. Balazs Z, Panzenboeck U, Hammer A, Sovic A, Quehenberger O, Malle E, et al. Uptake and transport of high-density lipoprotein (HDL) and HDL-associated alpha-tocopherol by an in vitro blood-brain barrier model. J Neurochem. 2004 May;89(4):939–50.

60. Bettens K, Vermeulen S, Van Cauwenberghe C, Heeman B, Asselbergh B, Robberecht C, et al. Reduced secreted clusterin as a mechanism for Alzheimer-associated CLU mutations. Mol Neurodegener. 2015;10:30.

61. Saeedi Saravi SS, Saeedi Saravi SS, Arefidoust A, Dehpour AR. The beneficial effects of HMG-CoA reductase inhibitors in the processes of neurodegeneration. Metab Brain Dis. 2017 Jun 3;

62. Calero M, Rostagno A, Matsubara E, Zlokovic B, Frangione B, Ghiso J. Apolipoprotein J (clusterin) and Alzheimer's disease. Microsc Res Tech. 2000 Aug 15;50(4):305–15.

63. Storck SE, Meister S, Nahrath J, Meißner JN, Schubert N, Di Spiezio A, et al. Endothelial LRP1 transports amyloid-β(1-42) across the blood-brain barrier. J Clin Invest. 2016 Jan;126(1):123–36.

64. Pietrzik CU, Busse T, Merriam DE, Weggen S, Koo EH. The cytoplasmic domain of the LDL receptor-related protein regulates multiple steps in APP processing. EMBO J. 2002 Nov 1;21(21):5691–700.

65. Oddo S, Caccamo A, Shepherd JD, Murphy MP, Golde TE, Kayed R, et al. Triple-transgenic model of Alzheimer's disease with plaques and tangles: intracellular Abeta and synaptic dysfunction. Neuron. 2003 Jul 31;39(3):409–21.

66. Lourenço CF, Ledo A, Barbosa RM, Laranjinha J. Neurovascular uncoupling in the triple transgenic model of Alzheimer's disease: Impaired cerebral blood flow response to neuronal-derived nitric oxide signaling. Exp Neurol. 2017 Feb 1;291:36–43.

67. Do TM, Alata W, Dodacki A, Traversy M-T, Chacun H, Pradier L, et al. Altered cerebral vascular volumes and solute transport at the blood-brain barriers of two transgenic mouse models of Alzheimer's disease. Neuropharmacology. 2014 Jun;81:311–7.

68. Panzenboeck U, Balazs Z, Sovic A, Hrzenjak A, Levak-Frank S, Wintersperger A, et al. ABCA1 and scavenger receptor class B, type I, are modulators of reverse sterol transport at an in vitro blood-brain barrier constituted of porcine brain capillary endothelial cells. J Biol Chem. 2002 Nov 8;277(45):42781–9.

69. Wahrle SE, Jiang H, Parsadanian M, Kim J, Li A, Knoten A, et al. Overexpression of ABCA1 reduces amyloid deposition in the PDAPP mouse model of Alzheimer disease. J Clin Invest. 2008 Feb;118(2):671–82.

70. Asztalos BF, Tani M, Schaefer EJ. Metabolic and functional relevance of HDL subspecies. Curr Opin Lipidol. 2011 Jun;22(3):176–85.

71. Olesen OF, Dagø L. High density lipoprotein inhibits assembly of amyloid beta-peptides into fibrils. Biochem Biophys Res Commun. 2000 Apr 2;270(1):62–6.

72. Kuo YM, Emmerling MR, Bisgaier CL, Essenburg AD, Lampert HC, Drumm D, et al. Elevated low-density lipoprotein in Alzheimer's disease correlates with brain abeta 1-42 levels. Biochem Biophys Res Commun. 1998 Nov 27;252(3):711–5.

73. Matsubara E, Frangione B, Ghiso J. Characterization of apolipoprotein J-Alzheimer's A beta interaction. J Biol Chem. 1995 Mar 31;270(13):7563–7.

74. Matsubara E, Soto C, Governale S, Frangione B, Ghiso J. Apolipoprotein J and Alzheimer's amyloid beta solubility. Biochem J. 1996 Jun 1;316 (Pt 2):671–9.

75. Koch M, Jensen MK. HDL-cholesterol and apolipoproteins in relation to dementia. Curr Opin Lipidol. 2016 Feb;27(1):76–87.

76. Barrett PJ, Song Y, Van Horn WD, Hustedt EJ, Schafer JM, Hadziselimovic A, et al. The amyloid precursor protein has a flexible transmembrane domain and binds cholesterol. Science. 2012 Jun 1;336(6085):1168–71.

77. Garner B. Lipids and Alzheimer's disease. Biochim Biophys Acta. 2010 Aug;1801(8):747–9.

78. Lingwood D, Simons K. Lipid rafts as a membrane-organizing principle. Science. 2010 Jan 1;327(5961):46–50.

79. Kojro E, Gimpl G, Lammich S, Marz W, Fahrenholz F. Low cholesterol stimulates the nonamyloidogenic pathway by its effect on the alpha -secretase ADAM 10. Proc Natl Acad Sci U S A. 2001 May 8;98(10):5815–20.

80. Ostrowski SM, Wilkinson BL, Golde TE, Landreth G. Statins reduce amyloid-beta production through inhibition of protein isoprenylation. J Biol Chem. 2007 Sep 14;282(37):26832–44.

81. Simons M, Schwärzler F, Lütjohann D, von Bergmann K, Beyreuther K, Dichgans J, et al. Treatment with simvastatin in normocholesterolemic patients with Alzheimer's disease: A 26-week randomized, placebo-controlled, double-blind trial. Ann Neurol. 2002 Sep;52(3):346–50.

82. Cordy JM, Hussain I, Dingwall C, Hooper NM, Turner AJ. Exclusively targeting beta-secretase to lipid rafts by GPI-anchor addition up-regulates beta-site processing of the amyloid precursor protein. Proc Natl Acad Sci U S A. 2003 Sep 30;100(20):11735–40.

83. Petanceska SS, DeRosa S, Olm V, Diaz N, Sharma A, Thomas-Bryant T, et al. Statin therapy for Alzheimer's disease: will it work? J Mol Neurosci MN. 2002 Oct;19(1–2):155–61.

84. Deane R, Bell RD, Sagare A, Zlokovic BV. Clearance of amyloid-beta peptide across the blood-brain barrier: implication for therapies in Alzheimer's disease. CNS Neurol Disord Drug Targets. 2009 Mar;8(1):16–30.

85. Ling I-F, Bhongsatiern J, Simpson JF, Fardo DW, Estus S. Genetics of clusterin isoform expression and Alzheimer's disease risk. PloS One. 2012;7(4):e33923.

86. Giannakopoulos P, Kövari E, French LE, Viard I, Hof PR, Bouras C. Possible neuroprotective role of clusterin in Alzheimer's disease: a quantitative immunocytochemical study. Acta Neuropathol (Berl). 1998 Apr;95(4):387–94.

87. Wang P, Chen K, Gu Y, Guo Q, Hong Z, Zhao Q. β-amyloid Upregulates Intracellular Clusterin but not Secretory Clusterin in Primary Cultured Neurons and APP Mice. Curr Alzheimer Res. 2017 May 30;

88. Merino-Zamorano C, Fernández-de Retana S, Montañola A, Batlle A, Saint-Pol J, Mysiorek C, et al. Modulation of Amyloid-β1-40 Transport by ApoA1 and ApoJ Across an in vitro Model of the Blood-Brain Barrier. J Alzheimers Dis JAD. 2016 May 25;53(2):677–91.

89. Cole GM, Beech W, Frautschy SA, Sigel J, Glasgow C, Ard MD. Lipoprotein effects on Abeta accumulation and degradation by microglia in vitro. J Neurosci Res. 1999 Aug 15;57(4):504–20.

90. Mulder SD, Nielsen HM, Blankenstein MA, Eikelenboom P, Veerhuis R. Apolipoproteins E and J interfere with amyloid-beta uptake by primary human astrocytes and microglia in vitro. Glia. 2014 Apr;62(4):493–503.

ABBREVIATIONS

AD: Alzheimer's Disease

Aβ: amyloid-beta peptide

ApoJ: apolipoprotein J

APP: amyloid precursor protein

BBB: blood-brain barrier

CAA: cerebral amyloid angiopathy

CSF: cerebrospinal fluid

CTF: C-terminal fragment

HPRT1: hypoxanthine phosphoribosyltransferase 1

ISF: interstitial fluid

LRP1: low-density lipoprotein receptor-related protein 1

mBCEC: primary murine brain capillary endothelial cells

pBCEC: primary porcine brain capillary endothelial cells

PGP: P-glycoprotein

RAGE: receptor for advanced glycation end products

TEER: transendothelial electrical resistance

TABLES

Gene	Sequence (5'-3')	Amplicon length (bp)
ssADAM10	F, AGCAACATCTGGGGACAAAC	219
	R, CTTCCCTCTGGTTGATTTGC	
ssAPP	F, CGTGGGAGTTTAGCTGCTTC	122
	R, TCAAATGCAATCGTGGAAAA	
ssAPOJ	F, CCTTCTTCGACATGATCCAC	282
	R, AGAGCTTGCTGAACTTCTCC	
ssBACE1	F, TGGACTGCCTCATGGTGTG	155
	R, GTGACCAAAGTGAACCACCG	
ssHPRT1	F, AGGACCTCTCGAAGTGTTGG	247
	R, CAGATGGCCACAGGACTAGA	
ssLRP1	F, GCAGATGTATCAACATCAACTGG	98
	R, GGGTGCTAGAGCAAGAGTGG	
ssLRP2	F, CATGTTTGTGTCCAGCCATC	191
	R, TCGTCACTTCCATCTCCACA	

ssPGP (MDR-1)	F, GAATTGCCCAGATAACAGCACCA	123
	R, GCCAGGCACCAGAACGAAAC	
ssRAGE	F, TCAAAACATCACAGCCCGGA	129
	R, GGAGTCAGGACCTTCCAAGC	
mmLRP1	F, CCGCATCTTCTTCAGTGACA	96
	R, ACAGAGCCCACATTTTCCAC	
mmRAGE	F, GGGAGGCCTGGGAGTAGTAG	92
	R, ATTCAGCTCTGCACGTTCCT	
mmAPP	F, TCCGAGAGGTGTGCTCTGAA	115
	R, CCACATCCGCCGTAAAAGAATG	
ssHMGR	F, CTTGTTCACGCGCACAGTCG	207
	R, GACAGCCAGAAGGAGAGCCA	
ssABCA1	F, GCCATTCTCCGGGCCAAC	252
	R, GGCTTCACGCCGCTGAT	
ssSREBP2	F, GCTTCTCCCCCTACTCCATC	151
	R, GAGAGGCACAGGAAGGTGAG	
mmHPRT1, mmLRP2	QuantiTect Primer Assay (Qiagen)	

Table 1: Primer sequences for porcine (ss) and murine (mm) genes used for real time PCR

siRNA	**Sequence (5'- 3')**	**Company**
ApoJ_1	5'- ACA GAU AAA GAC CCU AAU ATT -3'	Microsynth
ApoJ_2	5'- AUU UCC CGU GUG CCA CUA ATT -3'	Microsynth
ApoJ_3	5'- UUC CCU AUC ACU UCC CUG ATT -3'	Microsynth

Table 2: siRNA used for ApoJ silencing

FIGURES

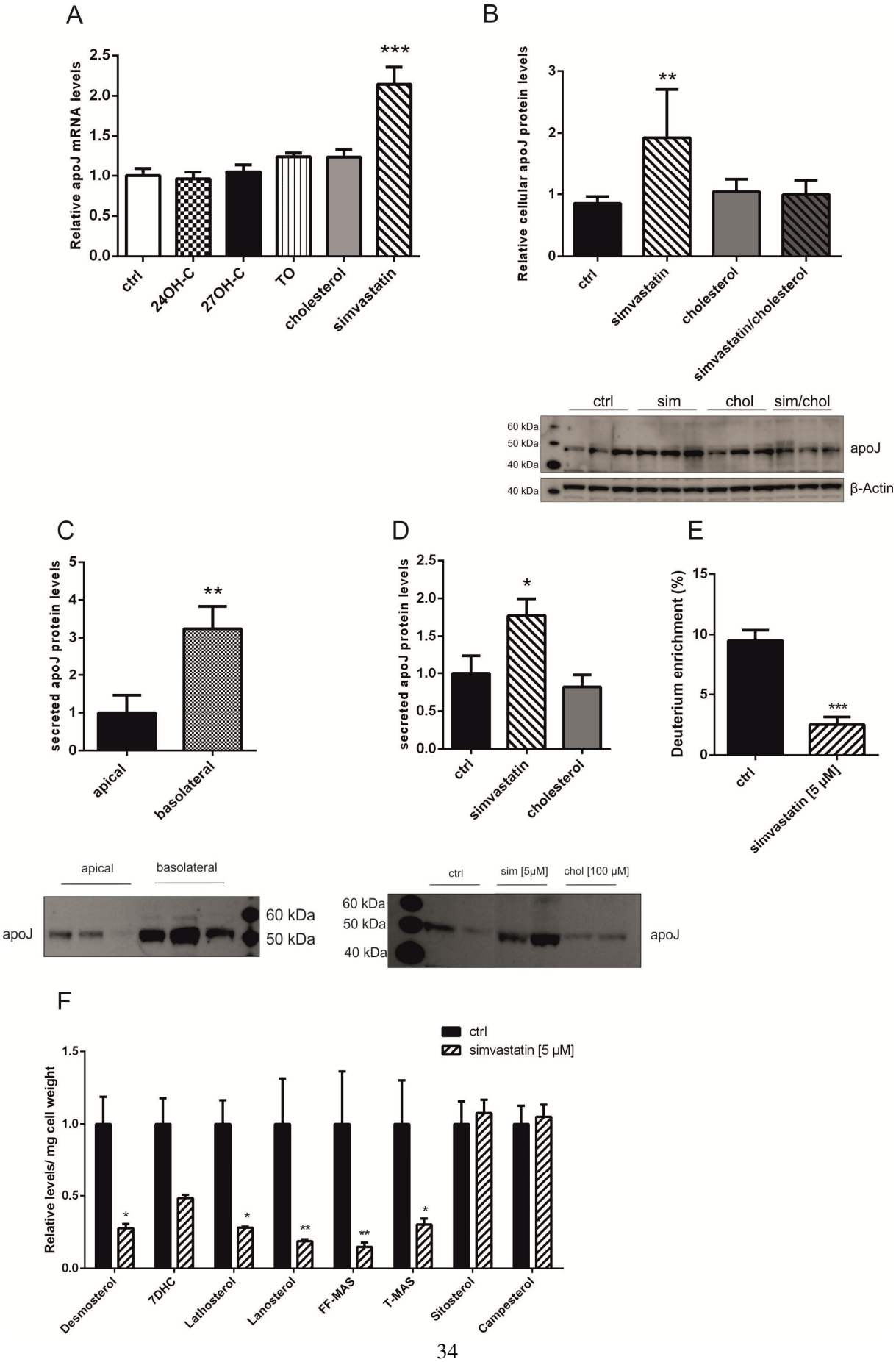
A
Relative apoJ mRNA levels
2.5
2.0
1.5
1.0
0.5
0.0
***
ctrl
24OH-C
27OH-C
TO
cholesterol
simvastatin
B
Relative cellular apoJ protein levels
3
2
1
0
**
ctrl
simvastatin
cholesterol
simvastatin/cholesterol
ctrl
sim
chol
sim/chol
60 kDa
50 kDa
40 kDa
apoJ
40 kDa
β-Actin
C
secreted apoJ protein levels
5
4
3
2
1
0
**
apical
basolateral
D
secreted apoJ protein levels
2.5
2.0
1.5
1.0
0.5
0.0
*
ctrl
simvastatin
cholesterol
E
Deuterium enrichment (%)
15
10
5
0
***
ctrl
simvastatin [5 µM]
apical
basolateral
apoJ
60 kDa
50 kDa
ctrl
sim [5µM]
chol [100 µM]
60 kDa
50 kDa
40 kDa
apoJ
F
ctrl
simvastatin [5 µM]
Relative levels/ mg cell weight
1.5
1.0
0.5
0.0
*
*
**
**
*
Desmosterol
7DHC
Lathosterol
Lanosterol
FF-MAS
T-MAS
Sitosterol
Campesterol

Fig. 1: Simvastatin increases mRNA and protein expression of apoJ in pBCEC. (A) Brain capillary endothelial cells were treated for 24 h in the absence (vehicle control) or presence of 10 µM 24OH-cholesterol (24OH-C), 10 µM 27OH-cholesterol (27OH-C), 2 µM TO, 100 µM cholesterol or 5 µM simvastatin. 0.5% ethanol in serum-free medium was used as vehicle control. Total RNA was isolated, reverse-transcribed and subjected to qPCR using SYBR green technology and HPRT1 as a reference gene. **(B)** pBCEC were incubated 24h in the absence (vehicle control) or presence of simvastatin [5µM], cholesterol [100 µM] and a combination of cholesterol and simvastatin. Western blot analysis of intracellular apoJ was performed using Rabbit-anti-clusterin antibody for detecting apoJ. **(C)** pBCEC were incubated on multiwell transwell filters to detect either apical ("blood compartment") or basolateral ("brain compartment") secretion of apoJ. **(D)** pBCEC were treated for 24 h with simvastatin [5µM] or cholesterol [100 µM] in serum-free medium and western blot analysis was performed from proteins precipitated from basolateral media. **(C,D)** Apical (1.5 ml) and basolateral (2.6 ml) media were collected, TCA-precipitated, and aliquots corresponding to 1 ml of supernatant and normalized to total cell cellular protein contents were subjected to immunoblot analysis using SDS-PAGE (4-12%) and PVDF membranes. The antibody Rabbit-anti-clusterin was used to detect secreted apoJ protein levels **(E)** To measure cholesterol synthesis, enrichment of deuterated water in the total cellular cholesterol fraction was determined using GC-MS analysis. All data represent mean±SD from 4 independent experiments performed in triplicates. **(F)** pBCEC were treated for 24 h with simvastatin [5 µM], or vehicle control (0.5% ethanol) and cellular lipids were isolated with Folch's solvent. Cholesterol precursors were measured using GC-MS analysis as described under Materials and Methods. Data represent mean±SD from 4 independent experiments performed in triplicates. *$p<0.05$; **$p<0.01$, ***$p<0.001$.

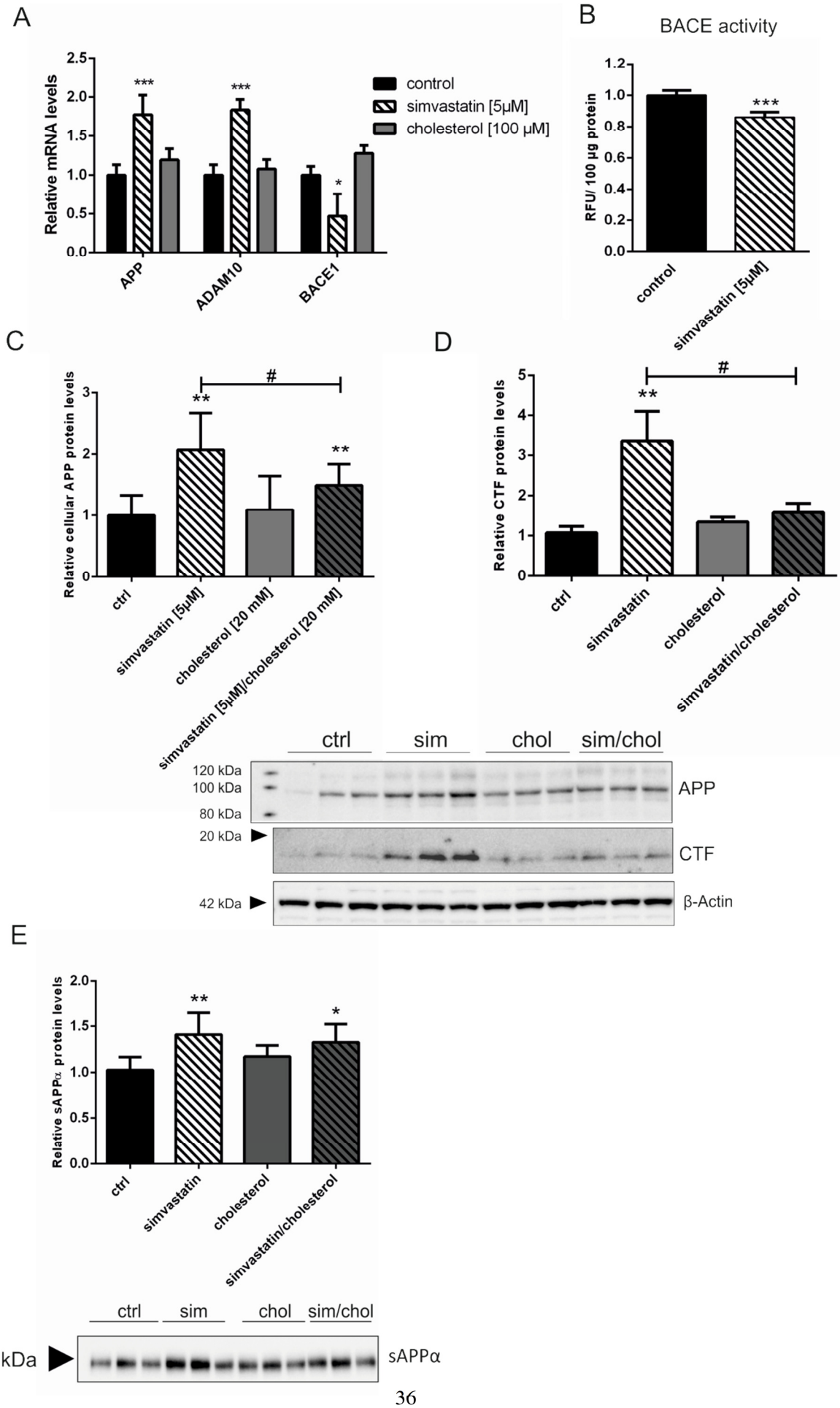
A
Relative mRNA levels
control
simvastatin [5μM]
cholesterol [100 μM]
APP
ADAM10
BACE1
B
BACE activity
RFU/ 100 μg protein
control
simvastatin [5μM]
C
Relative cellular APP protein levels
ctrl
simvastatin [5μM]
cholesterol [20 mM]
simvastatin [5μM]/cholesterol [20 mM]
D
Relative CTF protein levels
ctrl
simvastatin
cholesterol
simvastatin/cholesterol
ctrl
sim
chol
sim/chol
120 kDa
100 kDa
80 kDa
APP
20 kDa
CTF
42 kDa
β-Actin
E
Relative sAPPα protein levels
ctrl
simvastatin
cholesterol
simvastatin/cholesterol
ctrl
sim
chol
sim/chol
100 kDa
sAPPα

Fig. 2: Simvastatin affects APP expression and processing along with APP processing enzymes in pBCEC. Brain **c**apillary endothelial cells were treated for 24 h in presence of vehicle control [0.5% ethanol], cholesterol [100 µM], or simvastatin [5 µM], or a combination of cholesterol and simvastatin. **(A)** Total RNA was isolated, reverse-transcribed, and qPCR analysis was performed with CFX 96 real time system (Bio-Rad) using SYBR Green technology. mRNA expression levels were calculated using *ΔΔ*Ct method and HPRT1 as reference gene. Data represent mean±SD from 4 independent experiments. **(B)** Cell lysates of 100 µg protein were subjected to BACE1 activity assay kit provided by Abcam. Data represent mean±SD from 4 independent experiments performed in triplicates. **(C,D)** Immunoblot analysis was performed with extracted cell lysates and rabbit anti Amyloid Precursor Protein, C-Terminal antibody was used to detect APP and CTF (C-terminal fragments). Band intensities were evaluated densitometrically using β-actin for normalization. Blot is representative for one and data shown are mean±SD from 4 independent experiments performed in triplicates. # indicates significance ($p<0.05$) of simvastatin [5µM] as compared to combined treatment with simvastatin [5 µM] and cholesterol [100 µM]. **(E)** Media were collected, TCA-precipitated and subjected to western blot analysis was performed. Samples were normalized to total cellular protein and Anti-beta-Amyloid 1-16 (6E10) antibody was used for detecting sAPPα. Data represent mean±SD from 3 independent experiments performed in triplicates. *$p<0.05$; **$p<0.01$; ***$p<0.001$.

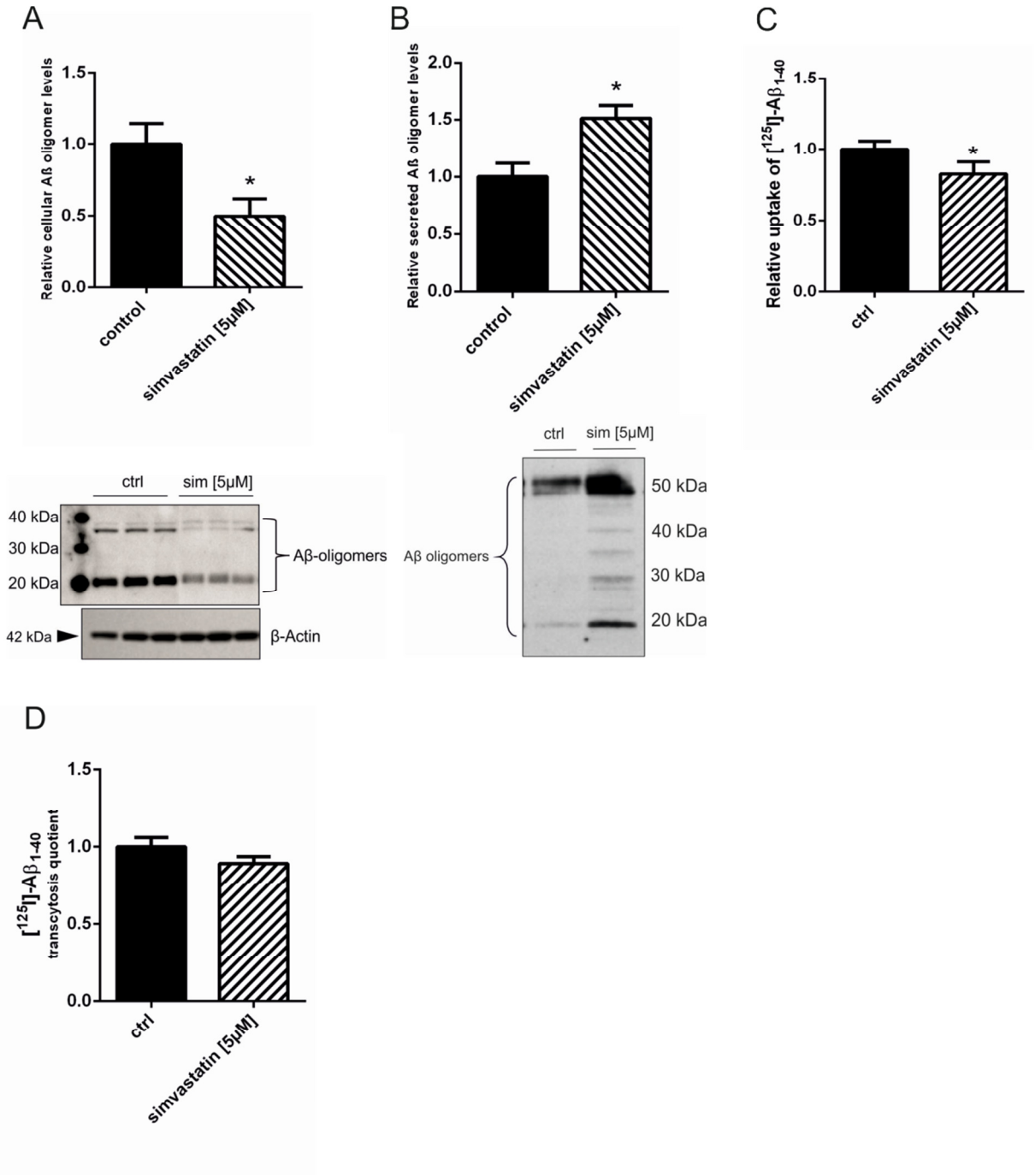

Fig. 3: Simvastatin treatment decreases cellular Aβ oligomers and Aβ uptake leaving extracellular Aβ oligomer levels increased. Brain capillary endothelial cells were incubated for 24 h in the presence or absence of simvastatin [5µM]. Ethanol [0.5%] was used as vehicle control. **(A**) Proteins from cell lysates were separated by SDS-PAGE and immunoblotting was performed using A11 rabbit-anti-amyloid oligomer antibody to detect cell-associated Aβ oligomers. Band intensities were evaluated densitometrically using β-Actin for normalization. **(B)** Extracellular proteins were TCA-precipitated from supernatants and aliquots were normalized to total cellular protein prior to immunoblot analysis. Secreted Aβ oligomers were detected using A11 rabbit-anti-amyloid oligomer antibody. **(A,B)** Blots shown

are representative for one and data represent mean±SD from 4 independent experiments. **(C)** pBCEC were cultured in the presence or absence of vehicle control or simvastatin [5µM]. Uptake assay was performed by incubating cells with [^{125}I]-A$\beta_{(1-40)}$ [0.3 nM] for 22 h. Data shown represent cpm/mg protein and mean±SD from 3 independent experiments performed in triplicates. **(D)** To examine the influence of an impaired cellular cholesterol metabolism on A$\beta_{(1-40)}$ transport across the BBB, pBCEC were split onto transwells, treated with simvastatin [5 µM] and [^{125}I]-A$\beta_{(1-40)}$ was added to the basolateral compartment. Transcytosis from the brain to the blood compartment was examined using radioactively labelled nucleotides. Data represent mean±SD from 3 independent experiments performed in triplicates. *$p<0.05$.

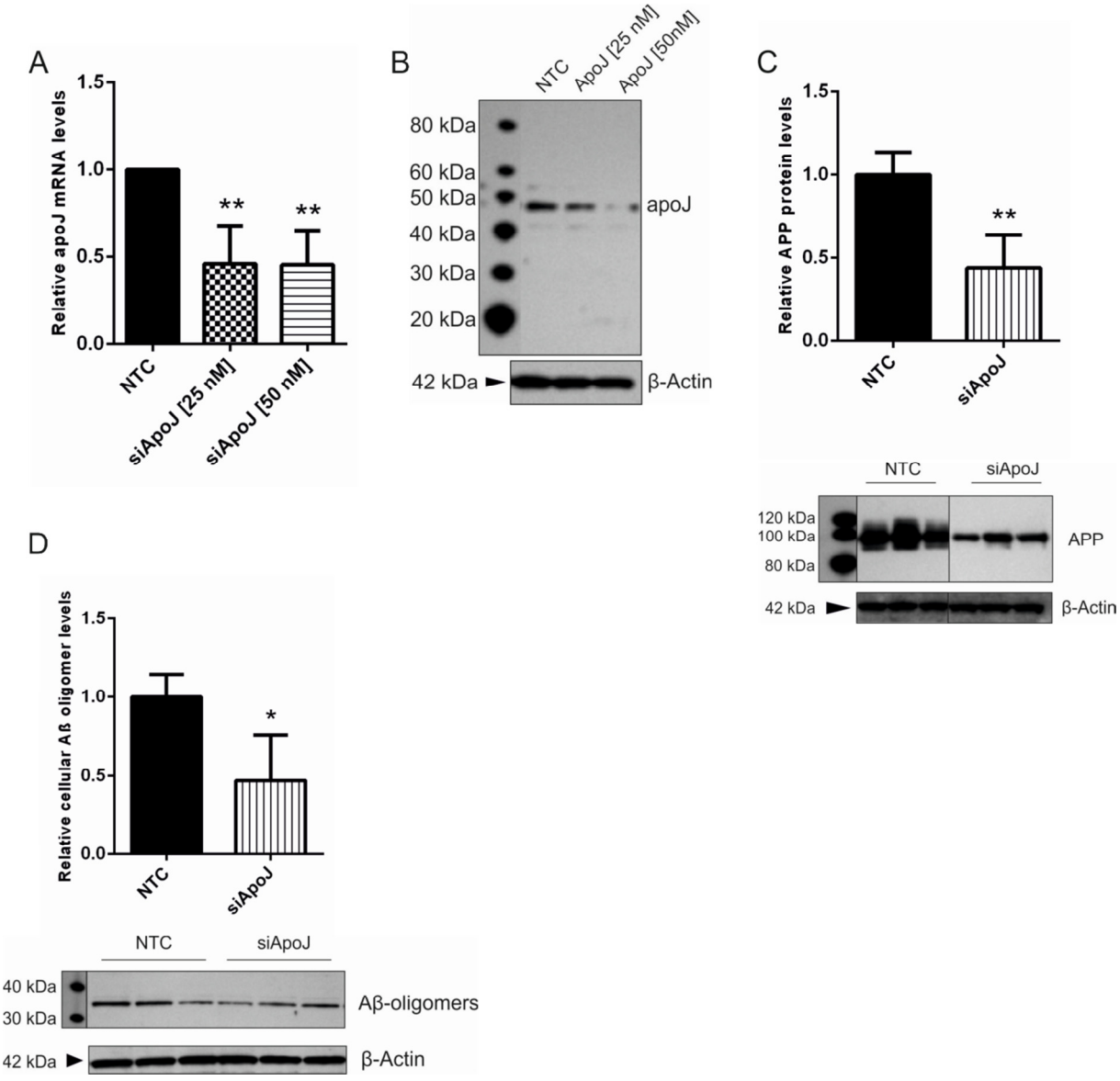

Fig. 4: Effects of apoJ silencing on APP and Aβ oligomers. (A) ApoJ was silenced by incubating pBCEC for 30 h with 25 nM or 50 nM siRNA. Scrambled siRNA was used as non-targeting control (NTC). **(B,C)** Immunoblot analysis was performed from extracted cell lysates. β-actin was used for normalization and densitometric evaluation. **(B)** ApoJ was detected using rabbit-anti-clusterin antibody. **(C)** Full-length APP was detected by using antibody rabbit-anti-β-APP. **(C,D)** Western blotting of APP and cellular Aβ oligomers was performed using extracts from cell lysates and rabbit-anti-β-APP and A11 rabbit-anti-amyloid oligomer antibodies. Data represent mean±SD from 4 independent experiments. *p<0.05; **p<0.01; ***p<0.001.

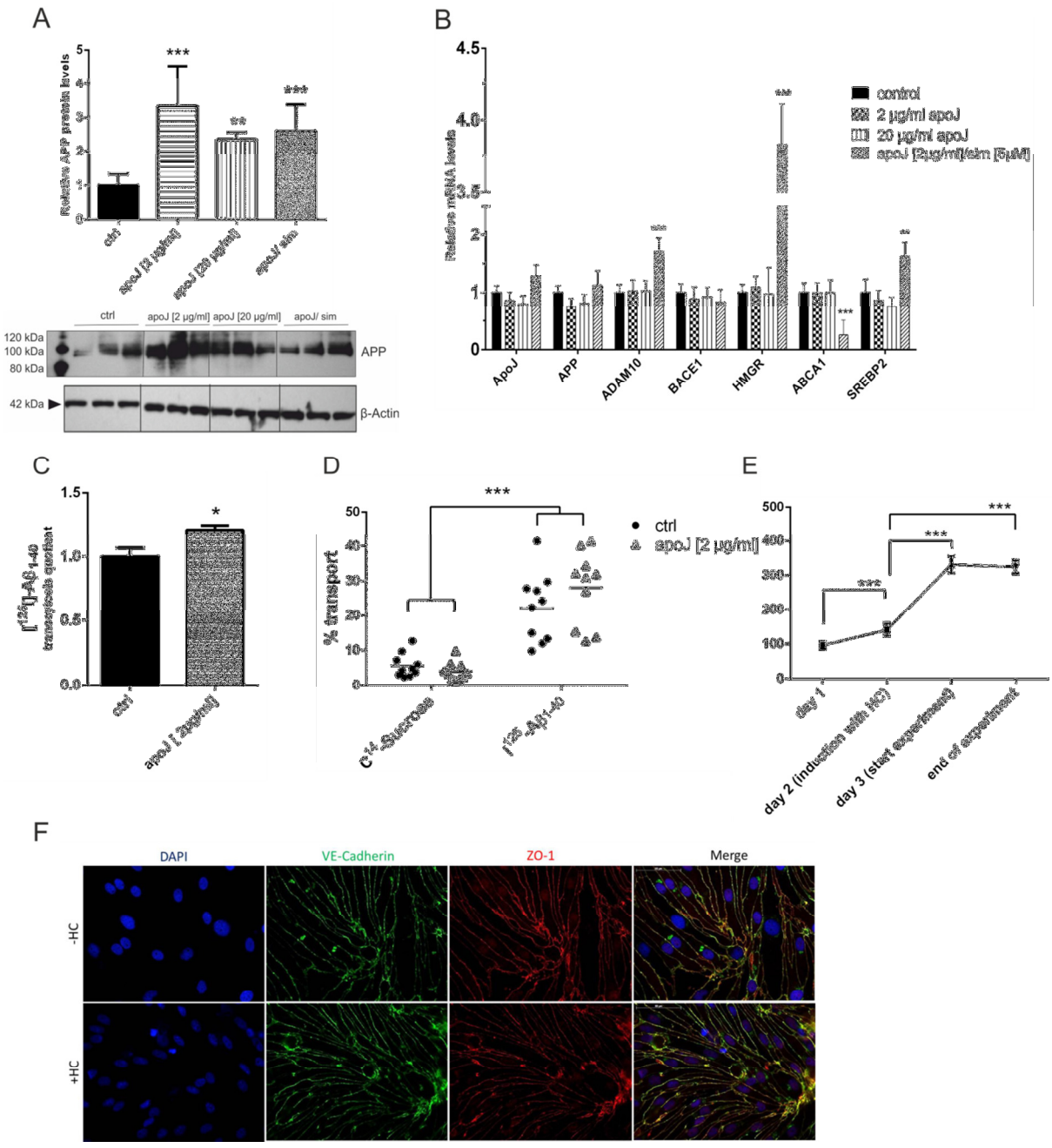

Fig. 5: Effects of addition of purified apoJ on APP and Aβ oligomer levels and transport. Cerebrovascular endothelial cells were treated for 24 h with 2 µg/ml or 20 µg/ml apoJ or a combination of apoJ [2 µg/ml] and simvastatin [5 µM]. **(A)** Immunoblot analysis was performed using rabbit-anti-β-APP antibody and β-actin for normalization. Data represent mean±SD from 4 independent experiments performed in triplicates. **(B)** Cells were harvested and RNA isolation and RT-qPCR was performed as described in Experimental procedures using *ΔΔCt* method. Data represent mean±SD from 3 independent experiments. (**C)** pBCEC were grown on transwell filters and treated with apoJ [2 µg/ml]. Transport was examined by adding [^{125}I]-A$\beta_{(1-40)}$ to the basolateral compartment and [^{14}C]-sucrose as a non-diffusion control. After 2 h incubation time, increase of A$\beta_{(1-40)}$ in the apical compartment was measured by using a γ-counter. Data represent mean±SD from 3 independent experiments

performed in triplicates. **(D)** Transport of [^{14}C]-sucrose and [^{125}I]-A$\beta_{(1-40)}$ from the basolateral to apical compartment of the endothelial barrier was measured after 2 h using a ß- and a γ-counter, respectively and data is shown in %. **(E)** Transendothelial electrical resistance (TEER) of pBCEC monolayers was measured using an EndOhm tissue resistance chamber and Evohm ohmmeter. On day 2 tight junction formation was induced incubating pBCEC with hydrocortisone [550 nM] for 24h. **(F)** Brain capillary endothelial cells were seeded on collagen G coated FlexiPerm slides, incubated in the absence or presence of hydrocortisone (HC, 550 nM, 24h) and immunofluorescently stained as described in Experimental procedures using anti-ZO1 (red) or anti-VE-cadherin (green) antibody. Cell nuclei were stained with DAPI (blue). Magnification: 63x. *$p<0.05$; **$p<0.01$; ***$p<0.001$.

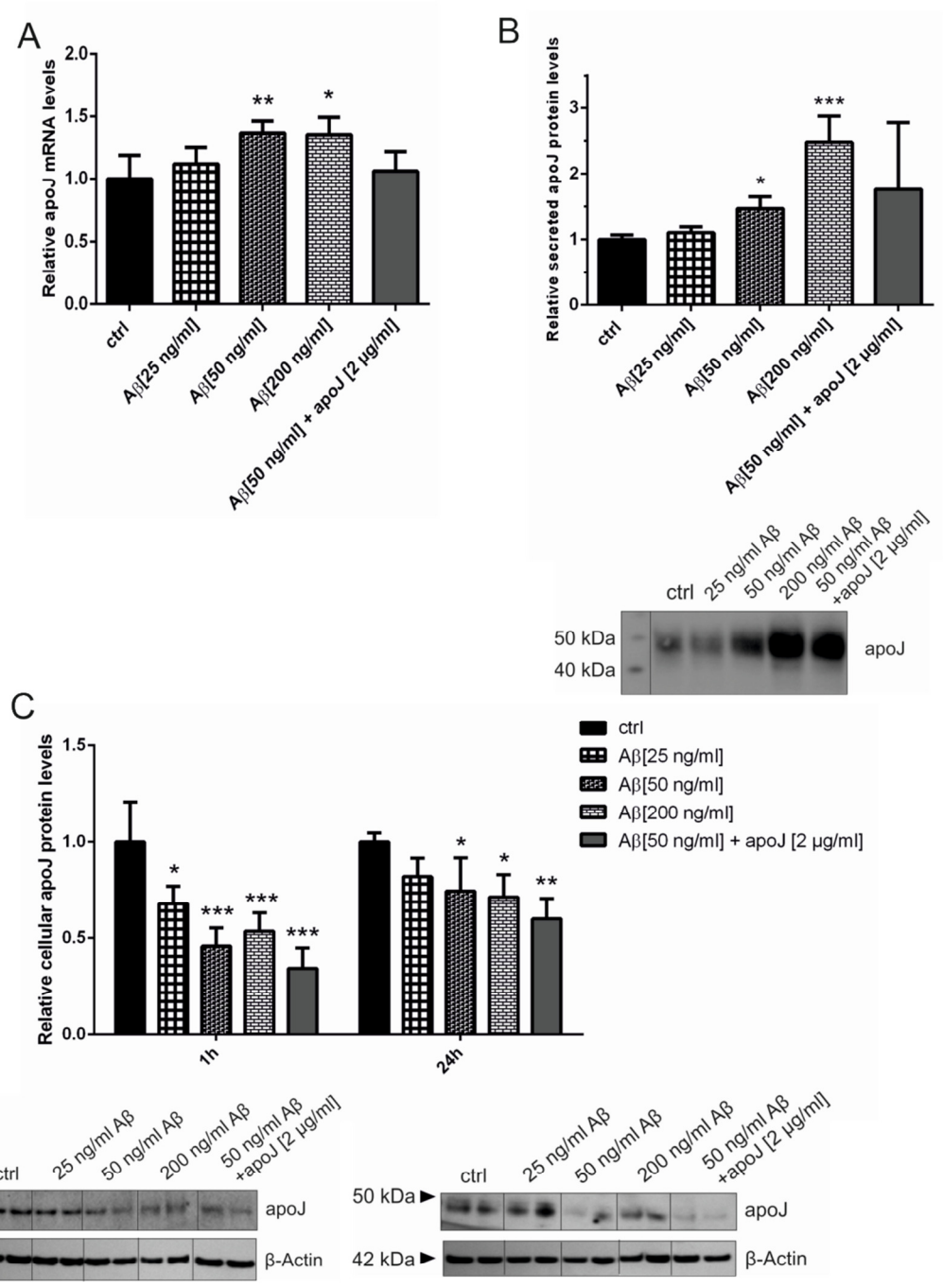
A
Relative apoJ mRNA levels
2.0
1.5
1.0
0.5
0.0
**
*
ctrl
Aβ[25 ng/ml]
Aβ[50 ng/ml]
Aβ[200 ng/ml]
Aβ[50 ng/ml] + apoJ [2 µg/ml]
B
Relative secreted apoJ protein levels
3
2
1
0
*
***
ctrl
Aβ[25 ng/ml]
Aβ[50 ng/ml]
Aβ[200 ng/ml]
Aβ[50 ng/ml] + apoJ [2 µg/ml]
ctrl
25 ng/ml Aβ
50 ng/ml Aβ
200 ng/ml Aβ
50 ng/ml Aβ +apoJ [2 µg/ml]
50 kDa
40 kDa
apoJ
C
Relative cellular apoJ protein levels
1.5
1.0
0.5
0.0
*
***
***
***
*
*
**
1h
24h
ctrl
Aβ[25 ng/ml]
Aβ[50 ng/ml]
Aβ[200 ng/ml]
Aβ[50 ng/ml] + apoJ [2 µg/ml]
ctrl
25 ng/ml Aβ
50 ng/ml Aβ
200 ng/ml Aβ
50 ng/ml Aβ +apoJ [2 µg/ml]
50 kDa
apoJ
42 kDa
β-Actin
ctrl
25 ng/ml Aβ
50 ng/ml Aβ
200 ng/ml Aβ
50 ng/ml Aβ +apoJ [2 µg/ml]
50 kDa
apoJ
42 kDa
β-Actin
D
absorbance A450 nm-A650 nm
0.6
0.4
0.2
0.0
ctrl
Aβ[25 ng/ml]
Aβ[50 ng/ml]
Aβ[200 ng/ml]

Fig. 6: $A\beta_{(1-40)}$ increases apoJ mRNA expression and mobilizes apoJ secretion by pBCEC. pBCEC were treated with increasing concentrations of $A\beta_{(1-40)}$ [25 ng/ml, 50 ng/ml, 200 ng/ml] or a combination of apoJ [2µg/ml] and $A\beta_{(1-40)}$ [50 ng/ml] for 1 h **(A,C)** and for 24 h **(B, C)**, respectively. **(A)** Total RNA was isolated, reverse-transcribed and gene expression analysis was performed using *ΔΔCt* method and normalization to *HPRT1*. **(B, C)** 15 µg of intracellular or secreted proteins –normalized to total cellular protein- were isolated from cell lysates and supernatants via TCA precipitation, respectively. Immunoblotting was performed using SDS-PAGE (4-12%) and PVDF membranes. β-Actin was used as loading control. Data represent mean±SD from 4 **(A, B)** and 5 **(C)** independent experiments. **(D)** $A\beta_{(1-40)}$ treatment does not influence cell viability. Cell viability test was performed using Cell Proliferation Reagent WST-1 by Roche. Data represent mean±SD (n=9) *p<0.05; **p<0.01; ***p<0.001.

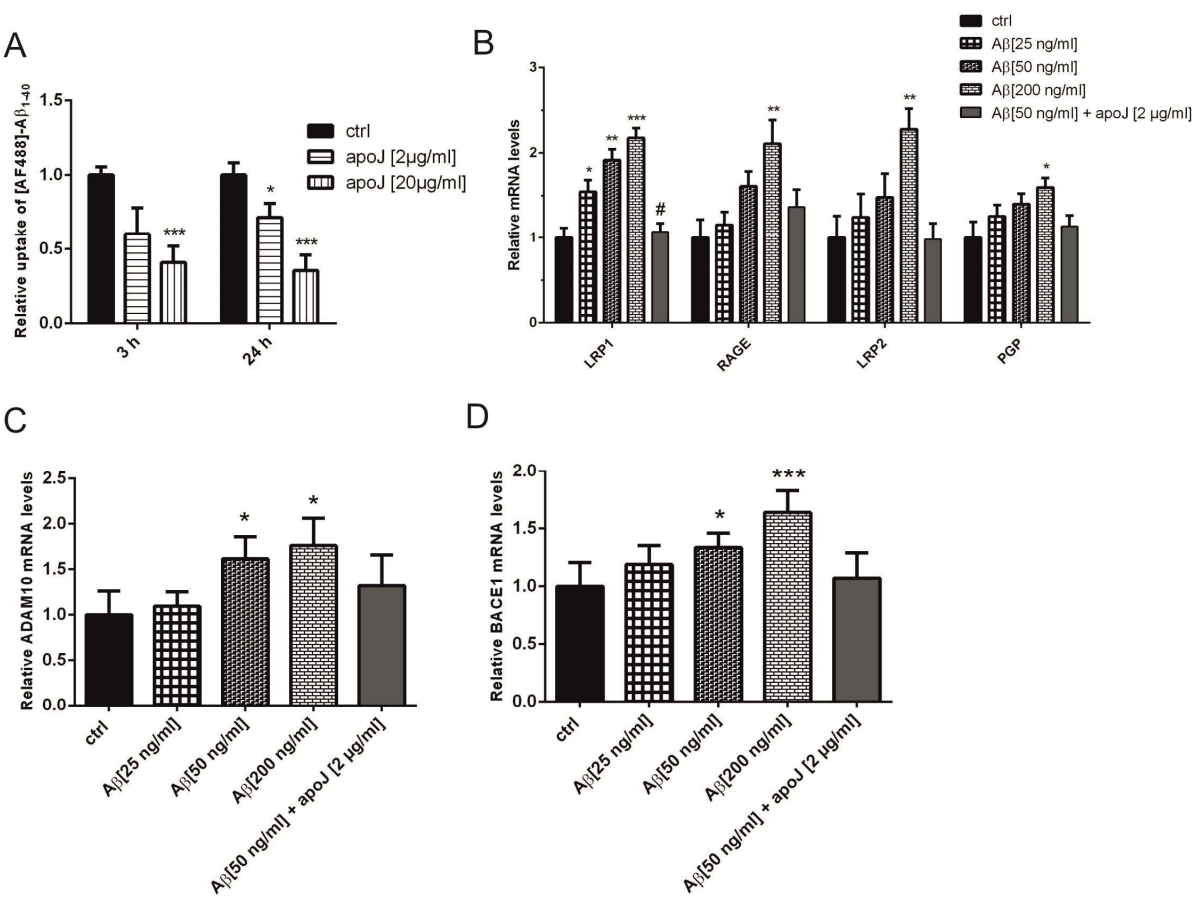

Fig. 7: ApoJ inhibits uptake of $A\beta_{(1-40)}$ by pBCEC and scavenges the effects of $A\beta_{(1-40)}$ on transcription of receptors known to be involved in amyloid transport. (A) Uptake assay was performed using Alexa Fluor 488 (AF488) labelled $A\beta_{(1-40)}$. pBCEC were incubated with AF488- $A\beta_{(1-40)}$ in the presence or absence of 2µg/ml and 20 µg/ml purified apoJ for 3h and 24h. Cells were lysed with 0.3 N NaOH and uptake was measured fluorescently using a fluorescent plate reader. Data represent mean±SD from 3 independent experiments performed in quadruplicates. **(B)** pBCEC were incubated for 1 h with increasing concentrations of $A\beta_{(1-40)}$ [25 ng/ml, 50 ng/ml, 200 ng/ml], or a combination of $A\beta_{(1-40)}$ [50 ng/ml] and apoJ [2 µg/ml]. RNA was isolated, and RT-qPCR was performed for low-density lipoprotein receptor-related protein 1 and 2 (LRP1, LRP2), receptor for advanced glycation end products (RAGE), and P-glycoprotein (PGP) using *ΔΔ*Ct method and HPRT1 as housekeeping gene. Data represent mean±SD from 4 independent experiments performed in triplicates. # indicates significance ($p<0.05$) of combined treatment with $A\beta_{(1-40)}$ [50 ng/ml] and apoJ [2 µg/ml] as compared to 50 ng/ml $A\beta_{(1-40)}$. **(C, D)** Total RNA was isolated, reverse-transcribed and qPCR analysis was performed for α-secretase (ADAM10) and β-secretase (BACE1) with CFX 96 real time system (Bio-Rad) using SYBR Green technology. mRNA expression levels were calculated using *ΔΔ*Ct method and HPRT1 as house-keeping gene.

Data represent mean±SD from 3 **(C)** and 5 **(D)** independent experiments performed in triplicates. *p<0.05; **p<0.01; ***p<0.001.

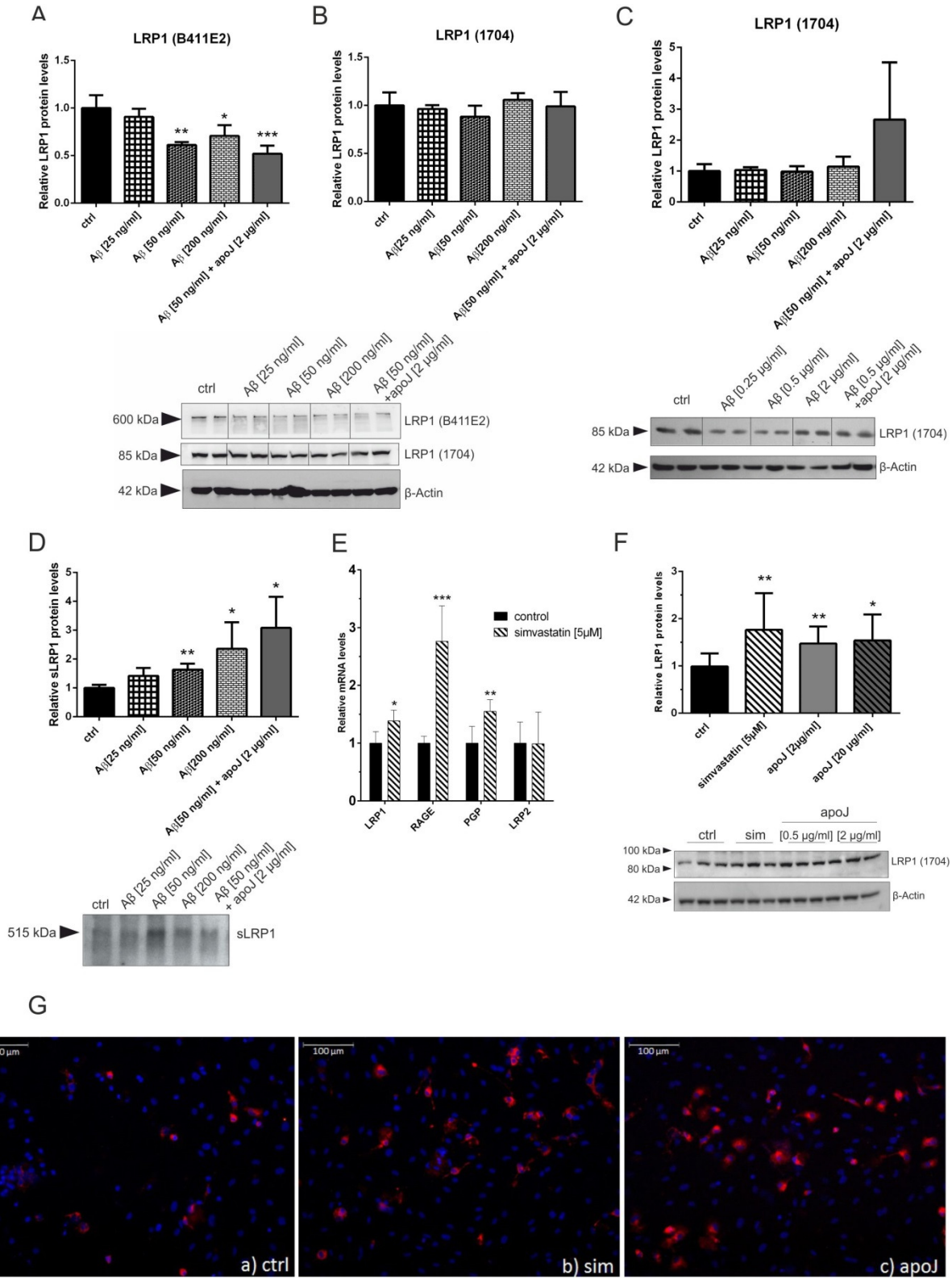

Fig. 8: Aβ$_{(1-40)}$ treatment increases sLRP1 protein levels in pBCEC. (A-C) To analyse protein levels of LRP1 α- and β-chain (B411E2) and the transmembrane domain (1704), pBCEC were treated for 1 h **(A,B)** and 24h **(C)** with increasing concentrations of Aβ$_{(1-40)}$ [25 ng/ml, 50 ng/ml, 200 ng/ml] or a combination of Aβ$_{(1-40)}$ [50 ng/ml]/apoJ [2 µg/ml]. Western blot analysis was performed after extracting proteins from cell lysates. β-Actin was used as

loading control and for normalization. Data represent mean±SD from 3 independent experiments. **(D)** Secreted, soluble LRP1 (sLRP1) protein levels were detected in the medium after 24 h incubation with increasing concentrations of $A\beta_{(1-40)}$. Antibody LRP1 (B411E2) was used to detect sLRP1. Aliquots loaded were normalized to total cellular protein. Data represent mean±SD from 5 independent experiments. **(E)** pBCEC were treated in the absence (0.5% Ethanol as vehicle control) and presence of simvastatin [5 µM] for 24h. RNA was isolated, reverse transcribed and subjected to RT-qPCR analysis. Data represent mean±SD from 5 independent experiments performed in triplicates. **(F)** Brain capillary endothelial cells were treated for 24h in the absence (0.5% Ethanol as vehicle control) and presence of simvastatin [5 µM] and apoJ [2 and 20 µg/ml]. Western blot was performed from intracellular protein using anti-Lrp1 (1704) antibody. Data represent mean±SD from 4 independent experiments performed in triplicates. **(G)** pBCEC were splitted on collagen G coated FlexiPerm Slides, treated with 5 µM simvastatin and 20 µg/ml apoJ and subjected to immunofluorescence microscopy using anti-rabbit-Lrp1 (1704) (red) as described in the Methods section. Cell nuclei were stained with DAPI (blue). Magnification: 20x *$p<0.05$; **$p<0.01$; ***$p<0.001$.

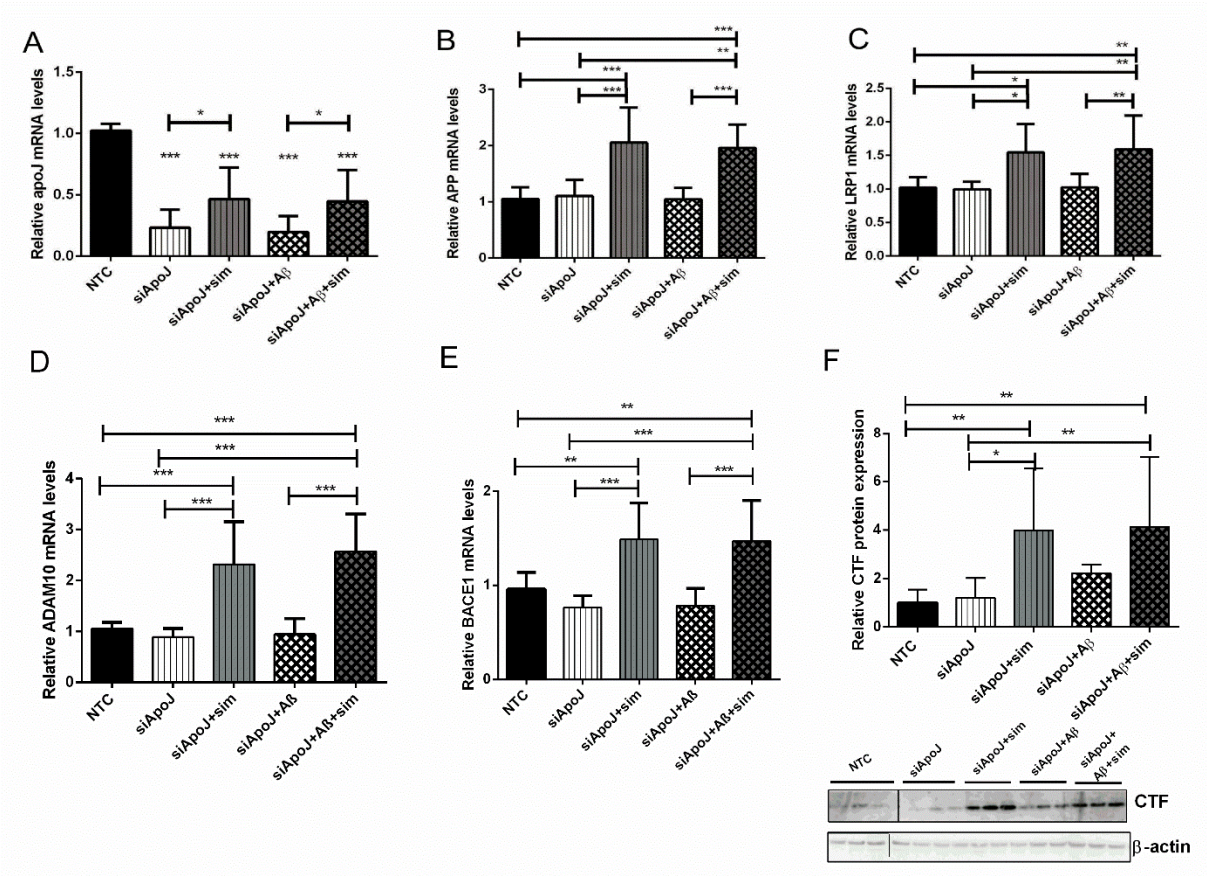

Fig. 9: Effects of simvastatin and Aβ treatment in apoJ silenced pBCEC. ApoJ was silenced by incubating pBCEC for 30 h with 50 nM siRNA. Scrambled siRNA was used as non-targeting control (NTC). In parallel, pBCEC were treated with simvastatin [5 µM] and/or $A\beta_{(1\text{-}40)}$ [50 ng/ml] as described in Methods. **(A-E)** Total RNA was isolated, reverse-transcribed, and qPCR analysis was performed with CFX 96 real time system (Bio-Rad) using SYBR Green technology. mRNA expression levels were calculated using *ΔΔ*Ct method and HPRT1 as reference gene. Data represent mean±SD from 3 independent experiments performed in triplicates. **(F)** Immunoblot analysis was performed with extracted cell lysates and rabbit anti Amyloid Precursor Protein, C-Terminal antibody was used to detect APP and CTF (C-terminal fragments). Band intensities were evaluated densitometrically using β-actin for normalization. Blot is representative for one and data shown are mean±SD from 3 independent experiments performed in triplicates. *p<0.05; **p<0.01; ***p<0.001.

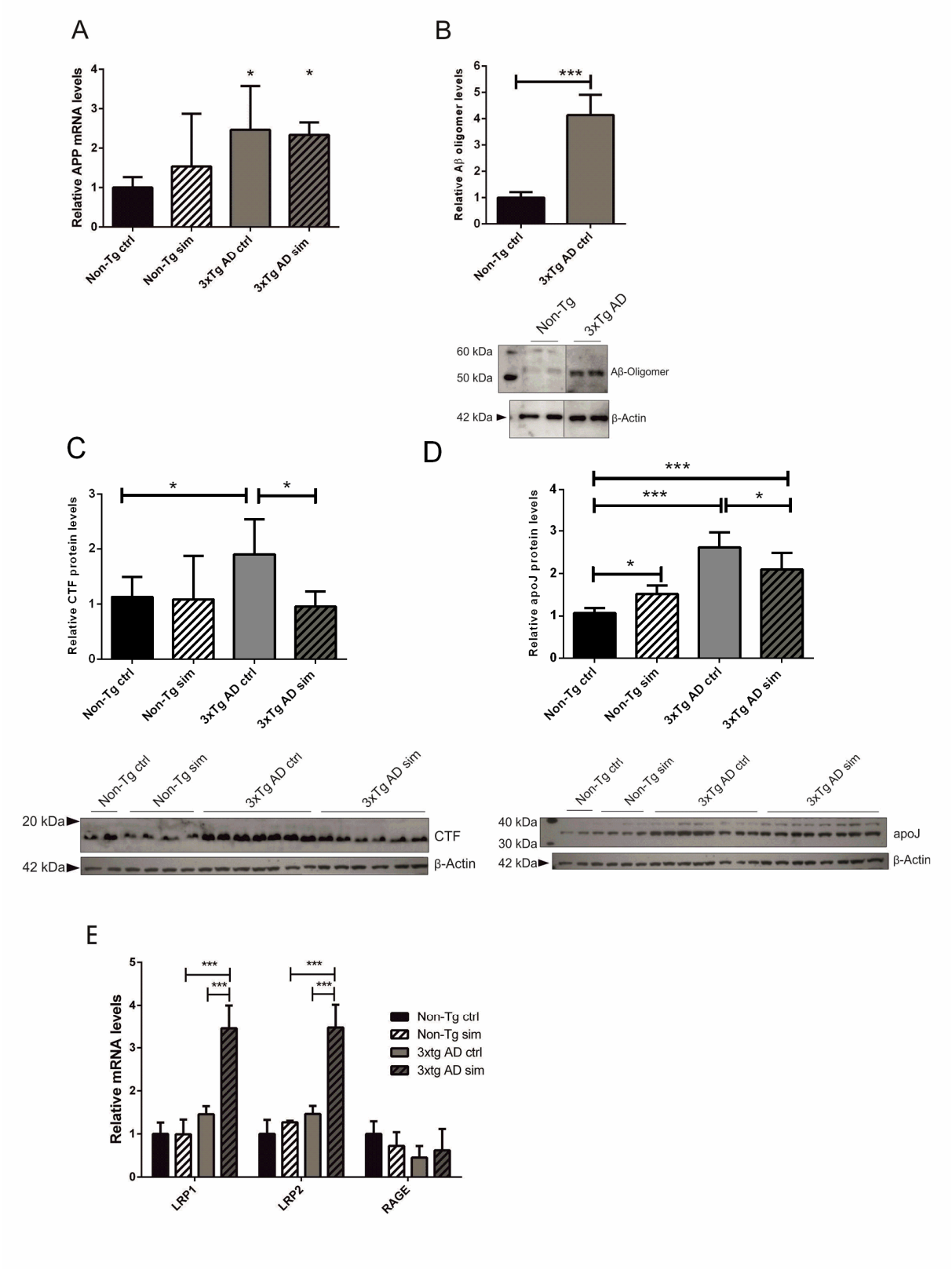

Fig. 10: Simvastatin (40 mg/kg) treatment *in vivo* affects APP processing, apoJ and LRP1 expression in BCEC. Female 3xTg AD mice and Non-Tg mice (aged 12 months and older) were daily gavaged for 21 days with 40 mg/kg simvastatin in 0.2% Agarose in PBS. **(A)** Relative mRNA levels of APP in whole brain were analysed by RT-qPCR using HPRT1

as housekeeping gene. **(B)** Western blot analysis of Aβ oligomer levels in mBCEC of 3xTg AD mice as compared to Non-Tg mice. β-Actin was used as loading control **(C, D)** Western blot analysis of C-terminal fragment (CTF) and cellular apoJ levels in 3xTg AD mice as compared to Non-Tg mice and to simvastatin treatment was performed with mBCEC using β-Actin as loading control and for normalization. (**E**) RNA was isolated from mBCEC, reverse-transcribed to cDNA. RT-qPCR analysis was performed for low-density lipoprotein receptor-related protein 1 and 2 (LRP1, LRP2) and receptor for advanced glycation end products (RAGE) using *ΔΔ*Ct method and HPRT1 as reference gene. All data represent mean±SD in mBCEC of a pool of hemispheres (Non-Tg mice: n=4; 3xTg AD mice: n=8). *$p<0.05$; **$p<0.01$; ***$p<0.001$.

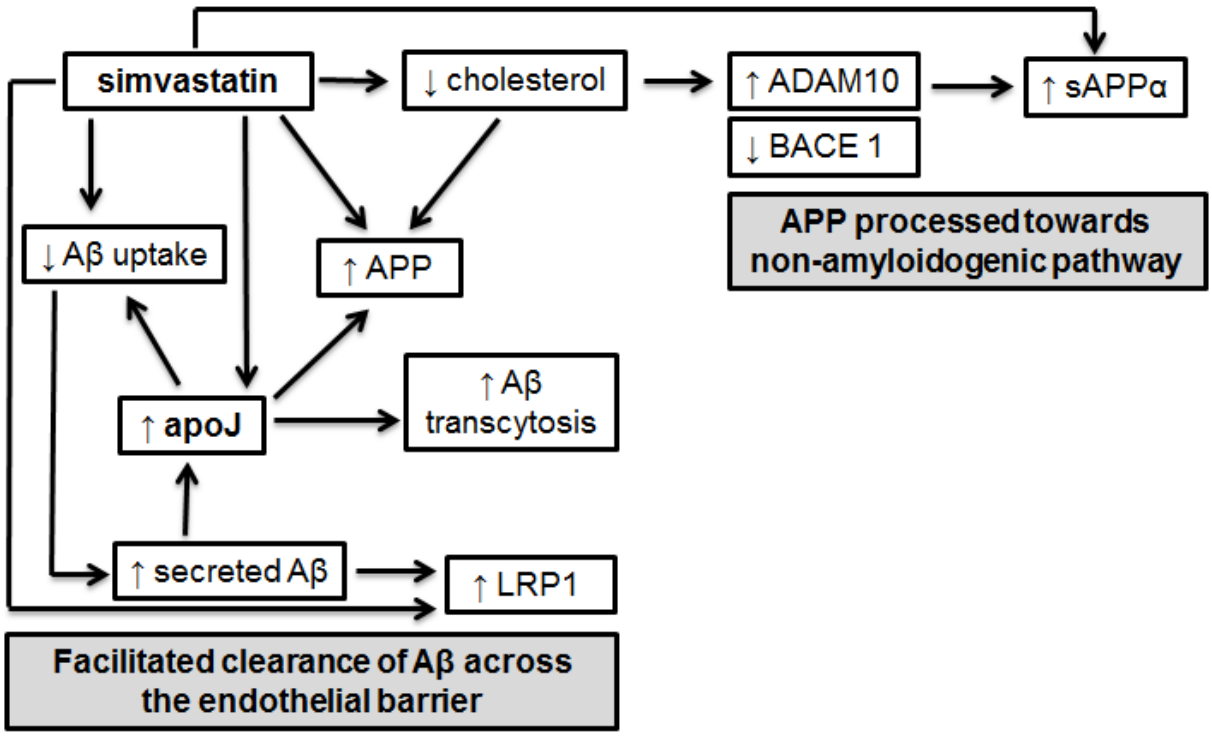

Fig. 11: Scheme depicting regulatory effects of simvastatin and apoJ at the BBB. Simvastatin, an inhibitor of cellular cholesterol synthesis, increases expression of the α-secretase ADAM10 and reduces expression and activty of the β-secretase BACE1, thereby shifting APP processing towards the non-amyloidogenic pathway. Further, simvastatin induces expression and secretion of apoJ predominantly to the basolateral compartment. Both, simvastatin and apoJ increase expression of APP and reduce Aβ uptake. In addition, apoJ facilitates transcytosis of Aβ from the basolateral to the apical compartment. Increased levels of Aβ in the cell surrounding as well as simvastatin induce expression of LRP1 and increase secretion of apoJ, faciliating thus processes leading to clearance of Aβ across the endothelial barrier.